



**JIMMA UNIVERSITY**  
**SCHOOL OF GRADUATE STUDIES**  
**JIMMA INSTITUTE OF TECHNOLOGY**  
**FACULTY OF CIVIL AND ENVIRONMENTAL ENGINEERING**  
**STRUCTURAL ENGINEERING STREAM**

**Finite Element Analysis of Concrete Filled Double Skin Steel Tubular  
Circular Column Subject to Axial Compression Loads.**

BY:

LEMZU MOHAMMED

A Thesis Submitted to the School of Graduate Studies of Jimma University in Partial Fulfillment of the Requirements for the Degree of Master Science in Civil Engineering. (Structural Engineering)

February, 2020

Jimma, Ethiopia

**JIMMA UNIVERSITY**  
**SCHOOL OF GRADUATE STUDIES**  
**JIMMA INSTITUTE OF TECHNOLOGY**  
**FACULTY OF CIVIL AND ENVIRONMENTAL ENGINEERING**  
**STRUCTURAL ENGINEERING STREAM**

**Finite Element Analysis of Concrete Filled Double Skin Steel Tubular  
Circular Column Subject to Axial Compression Loads**

BY:

LEMZU MOHAMMED

A Thesis Submitted to the School of Graduate Studies of Jimma University in Partial Fulfillment of the Requirements for the Degree of Master Science in Civil Engineering. (Structural Engineering)

Main Advisor: Engr. Elmer C Agon (Asso.prof)

Co-Advisor: Engr. Habtamu Gebremedhin (Msc)

February, 2020

Jimma Ethiopia

## DECLARATION

This thesis is my original work and has not been presented for a degree in any other university.

Thesis submitted by:

Lemzu Mohammed

Researcher

Signature

Date

This thesis has been submitted for examination with my approval as university supervisor.

Engr. Elmer C.Agon (Asso. Prof)

Main Advisor

Signature

Date

Engr. Habtamu Gebremedhin (Msc)

Co- Advisor

Signature

Date

### ACKNOWLEDGEMENT

My first foremost gratitude goes to Almighty Allah who is there for me always through the times of trouble and good times. Next I would like to express my sincere gratitude to my thesis advisor Engr. Elmer C. Agon (Asso.Prof) and my co-Advisor Engr. Habtamu Gebremedhin (Msc) for their valuable advice and guidance when I am preparing this thesis.

I would like to express my gratitude to all my families and friends for their encouragement and support in all situations. My special thanks go to Ethiopian roads Authority for facilitating this program which helps me for upgrading my profession. Last but not least, I am extremely and forever grateful to my wife Saliyat S. for her unrelenting and rigorous moral support not only on my educational careers but throughout my life.

## ABSTRACT

*Concrete filled double skin steel tubular circular (CFDSSTC) column is a creative innovation of steel-concrete composite construction, which are filled with concrete and supported by circular steel tubes on the interior and exterior. These steel tubes serve as formwork and hence these members are economical and quicker to construct when compared to conventional reinforced concrete columns. They are also efficient because they take advantage of the higher compressive strength of the concrete and high tensile strength of steel. CFDSSTC columns are proved to have good structural performance in terms of strength, stiffness, ductility and fire resistance.*

*This paper represents circular structural inner and outer steel tube filled with self-compacting concrete. Concrete filled double skin steel tubular circular (CFDSSTC) columns were modeled non-linearly by finite element method and analyzed in order to investigate the axial compression behavior of the specimens. The model of CFDSSTC column consisted of 3D solid elements to represent the inner and outer steel, concrete and, thick plate shell element to model the whole specimens.*

*The study proceeded by simulating of the model of the axial loads using Static, Riks non-linear finite element code. Different parametric studies were carried out. In the parametric studies, length of the column, hollowness ratio, internal and outer steel tubes thickness were taken as a parameter and the specimens were loaded in a concentric axial compression to investigate regarding their influence on the behavior of the columns. The result obtained from finite element analysis was carried out and verified with the experimental results obtained from the journal and used as a viable tool to expand the investigation into the axial behavior of CFDSSTC columns without having to conduct further expensive and time consuming tests. A parametric sensitivity analysis was performed using the validated finite element model to develop an in-depth understanding of the effects of various structure-related parameters on the impacts response of axially loaded CFDSSTC columns*

*Finally, the modeled columns were analyzed on ABAQUS 6.14 and their load displacement diagrams were drawn. The ultimate axial load capacities of all the columns were determined from these non-linear load-displacement curves. The study show that as the length and hollowness ration increase, the load resisting capacity of the column was decreased and there is an improvement on the behavior and axial load carrying capacity of concrete filled double skin steel tubular circular column due to the change in thickness of outer and inner steel tube. The strength of the column increase by 2.52% - 8.73% and 4.84% - 12.27% when the thickness of inner and outer steel tube thickness change from 2mm to 4mm respectively.*

*Keywords: CFDSSTC, Axial strength, inner and outer tube thickness, hollowness ratio, length of the column.*

## Table of contents

Contents	page
ACKNOWLEDGEMENT .....	ii
ABSTRACT.....	iii
List of Tables .....	vii
List of Figure.....	viii
Acronyms .....	x
List of Notations .....	xi
CHAPTER ONE .....	1
INTRODUCTION .....	1
1.1 Background of the study .....	1
1.2 Statements of the Problems .....	3
1.3 Objectives of the study .....	4
1.3.1 General objective .....	4
1.3.2 Specific objective .....	4
1.4 Research question.....	4
1.5 Significance of the study .....	5
1.6 Scope and limitation of the study .....	5
CHAPTER TWO .....	7
LITERATURE REVIEW .....	7
2.1 General.....	7
2.2 Types of concrete filled steel columns.....	8
2.3 Behavior of CFT column .....	10
2.4 CFDSSTC column under axial compression loads.....	11
2.5 Advantage and disadvantage of CFDSSTC columns .....	12
2.6 Structural behaviors of CFDSSTC columns .....	14
2.6.1 Effect of Confinement .....	14
2.6.2 Axial buckling.....	16
2.6.3 Bond between concrete and steel .....	18
2.6.4 Roles of steel tubes in composite columns.....	19
2.6.5 Load transfer mechanisms.....	20
2.6.6 Columns load capacity .....	21

2.6.7 CFDSSTC columns modes of failure .....	22
2.6.8 Buckling resistance.....	25
2.6.9 Stress-strain relationship for concrete core and steel tube .....	25
CHAPTER THREE .....	26
RESEARCH METHODOLOGY .....	26
3.1 General.....	26
3.2 Sample Detailing .....	26
3.3 Non-linear Finite element analysis .....	28
3.3.1 Parts (geometry) modeling .....	28
3.3.2 Part assembly and their interaction.....	30
3.3.3 Materials modeling of steel .....	31
3.3.4 Material modeling of concrete .....	32
3.3.5 Meshing.....	35
3.3.6 Analysis step.....	36
3.3.7 Boundary condition.....	36
3.3.8 Loading.....	37
3.4 study variables .....	38
3.4.1 Dependent variable:.....	38
3.4.2 Independent variable:.....	38
3.5 Sample size and sampling procedures .....	38
3.6 Data collection process. ....	38
3.6.1 Materials properties .....	38
3.7 Data processing and analysis .....	39
3.8 Data quality assurance.....	39
3.9 Validation of the model .....	39
CHAPTER FOUR.....	41
RESULT AND DISCUSSION .....	41
4.1 Effects of hollowness ratio on the behavior of CFDSSTC columns. ....	41
4.2 Effects of outer steel tube thickness on the behavior of CFDSSTC columns. ....	43
4.3 Effects of inner steel tube thickness on the behavior of CFDSSTC columns.....	45
4.4 Effects of length of the columns on the behavior of CFDSSTC columns.....	47
4.5 Modes of failure.....	49
CHAPTER FIVE .....	51

CONCLUSION AND RECOMMENDATION ..... 51

    5.1 Conclusion..... 51

    5.2 Recommendation..... 53

REFERENCE..... 54

APENDIX A ..... 58

MATERIAL PROPERTIES ..... 58

APENDEX B ..... 61

Axial loads for all CFDSSTC columns..... 61



## List of Tables

	Page
Table 2.1: Axial load resisting performance of different outer and inner tube thickness [30].	20
Table 3.1: Analyzing program and CFDSSTC specimen's details.	26
Table 3.2: Properties of steel.	32
Table 3.3: Properties of concrete.	34
Table 4.1: Load and Displacement data for (CFST-2, CFST-3, CFST-4, CFST-5, and CFST-6).	41
Table 4.2: Axial load capacity of the specimens (for CFST-4 to CFST-8).	42
Table 4.3: Load Displacement data for columns (CFST-12 to CFST-16).	43
Table 4.4: Axial load capacity of the specimens (CFST-12 TO CFST-16).	44
Table 4.5: Load and displacement data for specimens (increasing inner steel tube thickness).	45
Table 4.6: Axial load capacity of the specimens for inner steel tube thickness.	46
Table 4.7: Ultimate load capacity of the specimens with increasing length of the column.	47
Table 4.8: Load-Displacement data for the specimens (increasing length of the column).	49
Table A.1: Compressive stress-total strain of concrete.	58
Table A.2: Compressive stress-crushing strain.	58
Table A.3: Concrete damage variable vs crushing strain.	58
Table A.4: Tensile stress-cracking strain of concrete.	59
Table A.5: Tensile damage variables-cracking strain of concrete.	60

## List of Figure

	Page
Figure 1.1: Cross sectional view of hollow steel column in-filled with concrete [1].	2
Figure 2.1: Typical cross section of composite columns ( Ermiyas Ketema, A.A University thesis).	9
Figure 2.2: CFDSSTC columns details [14], a) cross section, b) longitudinal section.	12
Figure 2.3: Idealized column buckling curve (a), non-dimensionalized column buckling curve (b).	17
Figure 2.4: Schematic failure modes of hollow steel tube, concrete and CFST stub columns [34].	24
Figure 3.1: Plain concrete part for the first column.	29
Figure 3.2: Steel column part for the first column.	29
Figure 3.3: Loading steel plate part for the first column.	30
Figure 3.4: Assembled CFDSSTC column using ABAQUS for the first column.	30
Figure 3.5: Elastic perfectly plastic model for steel tube [37].	32
Figure 3.6: Uniaxial stress-strain curves for confined and unconfined concrete.	33
Figure 3.7: Finite element mesh for one of the CFDSSTC column analyzed.	35
Figure 3.8: Boundary condition for one of CFDSSTC column analyzed.	37
Figure 4.1: Load -Displacement curve for column (CFST-2 to CFST-6).	42
Figure 4.2: Load-Displacement curve for increasing outer steel tube thickness.	44
Figure 4.3: Load-Displacement curve for the specimens (increasing inner steel tube thickness).	46
Figure 4.4: Load-Displacement curve for column with increasing length.	48
Figure 4.5: Failure on OST=3mm specimens.	50
Figure 4.6: Failure on 0.6mm specimens.	50
Figure 4.7: Failure on HR=1 CFDSSTC columns.	50
Figure B.1: Axial loads for HR=0 columns.	61
Figure B.2: Axial loads for HR=0.25 CFDSSTC columns.	61
Figure B.3: Axial loads for HR=0.5 CFDSSTC columns.	62
Figure B.4: Axial loads for HR=0.75 CFDSSTC columns.	62
Figure B.5: Axial loads for HR=1 CFT columns.	63
Figure B.6: Axial loads for IST=2mm CFDSSTC column.	63
Figure B.7: Axial loads for IST=2.5mm CFDSSTC column.	64
Figure B.8: Axial loads for IST=3mm CFDSSTC column.	64
Figure B.9: Axial loads for IST=3.5mm CFDSSTC column.	65
Figure B.10: Axial loads for IST=4mm CFDSSTC column.	65
Figure B.11: Axial loads for OST=2mm CFDSSTC column.	66
Figure B.12: Axial loads for OST=2.5mm CFDSSTC column.	66
Figure B.13: Axial loads for OST=3mm CFDSSTC column.	67
Figure B.14: Axial loads for OST=3.5mm CFDSSTC column.	67
Figure B.15: Axial loads for OST=4mm CFDSSTC column.	68
Figure B.16: Axial loads for L=1m CFDSSTC column.	68
Figure B.17: Axial loads for L=1.5m CFDSSTC column.	68
Figure B.18: Axial loads for L=2m CFDSSTC column.	69
Figure B.19: Axial loads for L= 2.5m CFDSSTC column.	69
Figure B.20: Axial loads for L= 3m CFDSSTC column.	70
Figure B.21: Axial loads for L=3.5m CFDSSTC column.	70

---

Figure B.22: Axial loads for L=4m CFDSSTC column. .... 71  
Figure B.23: Axial loads for 0.6m CFDSSTC column. .... 71

## Acronyms

3D	Three Dimensional
CFDSSTC	Concrete Filled Double-Skin Steel Tubular Circular
CFST	Concrete Filled Steel Tube
EBCS	Ethiopian Building Code Standards
FEA	Finite Element Analysis
FE	Finite Element
HSS	Hollow Structural Steel
RC	Reinforced Concrete
RCC	Reinforced Concrete Column
SCC	Self-Compacting Concrete
$\chi$	Hollowness ratio

## List of Notations

$A_C$	Area of concrete section
$A_{it}$	Cross sectional area of inner steel tube
$A_{ot}$	Cross sectional area of outer steel tube
$D_i$	Diameter of inner steel
$D_O$	Diameter of outer steel
$E_{cm}$	Secant modulus of elasticity of concrete
$(EI)_e$	Bending stiffness of the column
$E_S$	Elastic modulus of steel
$F_{ck}$	Characteristic strength of concrete
$F_{cm}$	Mean Compressive strength at 28 days
$f_{it}$	Axial stress of the inner steel tube
$f_{ot}$	Axial stress of the outer steel tube
$f_y$	Yield strength of steel
$L$	Length of the Column
$N_{cr}$	Elastic modulus of steel
$t_i$	Thickness of inner steel tube
$t_o$	Thickness of outer steel tube

## CHAPTER ONE

### INTRODUCTION

#### 1.1 Background of the study

Composite steel-concrete construction has become a widespread solution in modern construction. It ideally combines the advantage of both steel and concrete, namely fast construction, high strength and light weight of steel together with inherent mass, stiffness, damping and economy of concrete. A creative innovation of composite steel-concrete construction is the concrete-filled double skin steel tube (CFDSST), which is formed by two concentric steel tubes separated by concrete filler.

Due to the excellent composite action between the steel tubes and concrete, concrete-filled double skinned steel tubular (CFDSST) columns are becoming increasingly popular and used in various structures throughout the world.

The concrete filled steel tube (CFST) structural system is a system based on filling steel tubes with high-strength concrete. It is one of the modifications to composite steel-concrete structures. CFST structure is a type of the composite steel-concrete structures used presently in civil engineering and consists of steel tube and concrete core inside it. Combining the advantage of both hollow structural steel (HSS) and concrete, concrete filled steel tubes (CFST) are being used widely in real civil engineering projects due to their excellent static and earthquake resistant properties, such as high strength, high ductility and large energy absorption capacity. Concrete filled steel tubes (CFST) are also used extensively in other modern civil engineering applications. When they are used as structural columns, especially in high-rise buildings, the composite members may be subjected to high shearing force as well as moments under wind or seismic actions [1].

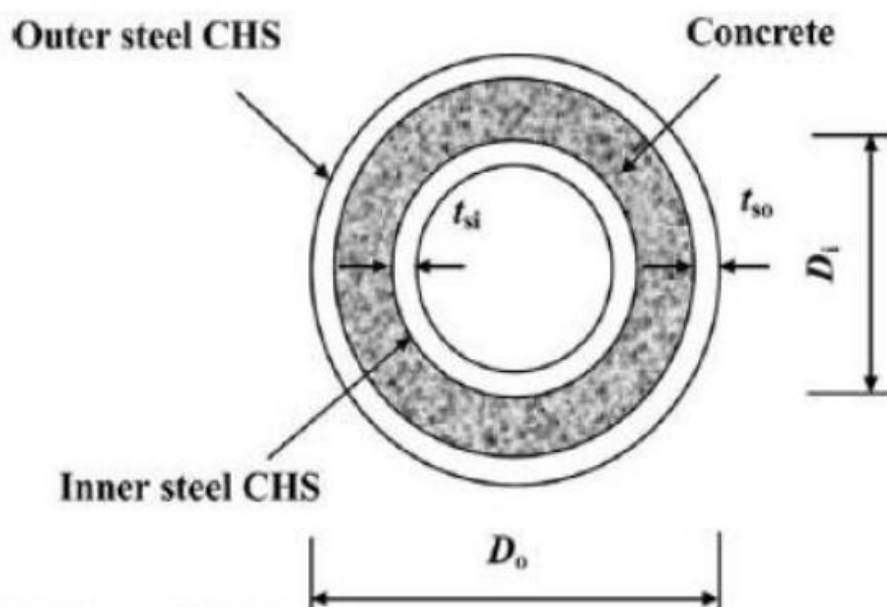


Figure 1.1: Cross sectional view of hollow steel column in-filled with concrete [1].

In composite construction, the concrete and steel are combined in such a fashion that the advantages of both the materials are utilized effectively in composite column. The lighter weight and higher strength of steel permit the use of smaller and lighter foundations. The subsequent concrete addition enables the building frame to easily limit the sway and lateral deflections. Hollow column has less self-weight and a high flexural stiffness and hence its usage in seismic zone proves promising. It reduces requirement on formwork, labor, construction time, and maintains the construction quality. It also provides spaces for facilities such as power cables, drainage pipes and telecommunication line where needed. The presence of concrete core in a CFDSSTC can effectively restrain and delay local buckling of the steel tubes. The tubes act as longitudinal reinforcement, provide a confining effect for the concrete and control the damage of the concrete. The synergy between the tubes and concrete core results in a more redundant section which completely fails only when all three layers of materials fail. These members are economical and quicker to construct when compared to conventional reinforced concrete (RC) members as the tubes serve as the permanent form work. A CFDSSTC member requires a smaller cross sectional area; hence less self-weight, to achieve the same axial or bending capacity compared to RC members. Additionally, isolation of concrete core by the tubes, reduce concrete maintenance requirements.

## 1.2 Statements of the Problems

Concrete filled steel tube columns have been adopted widely for column construction of tall buildings due to its excellent confining effect. However, the central part of concrete in CFST columns have relatively high cross sectional area, which can be effectively replaced by another hollow steel tube with much smaller area without reducing the load carrying capacity due to composition action. This structural form with the in-between annulus of inner and outer steel tubes filled with concrete is called concrete-filled double-skin steel tubular circular (CFDSSTC) columns. Nonetheless, similar to CFST columns, the imperfect steel-concrete interface bonding of the outer tube will take place in the initial elastic stage because steel dilates more than concrete. It consequently reduces the confinement and stiffness of the CFST columns [2].

Several studies have been conducted to investigate the strength of concrete filled double-skin steel tubular circular (CFDSST) short columns under axial compression and bending loads. However, very few studies have been conducted on long columns to investigate their axial load resisting performance. These studies are limited in scope and their conclusions are preliminary. They lack experimental insight into the response of CFDSSTC members when used as structural columns subjected to axial load induced by live and dead loads of building slabs or bridge decks. Additionally, from a through literature search, no reference was found on the use of a validated finite element model to simulate the load resisting performance of axially loaded CFDSSTC columns [3].

Therefore, it is necessary to establish a systematic research program to examine the structural response of both short and long CFDSSTC columns under axial compression loading, characterizing their potential to mitigate the risk from failure and collapse of columns under axially compression loading and generate information on the effects of controlling parameters through an experimental study and a parametric study using a validated numerical model, which can adequately replicate the response of such columns.



### 1.3 Objectives of the study

#### 1.3.1 General objective

The general objective of this thesis was to assess the axial compressive behavior of concrete filled double skin steel tubular circular (CFDSSTC) columns.

#### 1.3.2 Specific objective

The specific objectives of this research are:

- ✓ To investigate the influence of parameters such as hollowness ratio, length of the column (L) and thickness of the outer and inner steel tubes on ultimate load carrying capacity of the columns.
- ✓ To give a numerical base of information for the design of circular columns consisting of concrete filled hollow steel sections.
- ✓ To develop a numerical model in order to simulate the behavior of concrete filled double skin steel tubular circular (CFDSSTC) columns under axial loading.

### 1.4 Research question

In order to achieve the aim of this research, the following question are posed

- ✓ What are the appropriate numerical techniques which should be employed to be able to create a robust and efficient finite element model that can be accurately simulate and predict the response of axially loaded CFDSSTC columns?
- ✓ What should be the key load and structure-related parameters and what should be the response parameters?
- ✓ Can the information generated through this research be analyzed and the outcome is presented through graphs?
- ✓ Does the length of the column are the cause of failure of CFDSSTC column?
- ✓ What programs or tool can be developed to be used in practical situations to increase the axial load carrying capacity of CFDSSTC columns?

### 1.5 Significance of the study

This research tried to contribute the proper understanding of the axial behavior of concrete filled double-skin steel tubular circular columns and possible cause of failure on building due to columns properties; this may lead to one of the correct application of remedial measures.

The study motivate those who are interested to conduct further research on axial behavior of concrete filled double-skin steel tubular circular columns and the result should be of interest to engineers considering the use of such columns in various structural applications. Practical use of double skin steel tubular circular (CFDSSTC) columns requires knowledge of the basic compressive behavior of the concrete as well as knowledge of the interrelationship between stress and strain. The research discussed here in focuses on determining the basic behavior and defining the interrelationships.

An advanced finite element model of CFDSSTC columns subject to axial load was developed which show to be valid, with excellent correlation with the experimental result obtained from the journal. This validated model can be used as a viable tool in analyzing or designing the CFDSSTC columns under axial load. This research also provided new information on the influence of important structural and related variables on the key response parameters of CFDSSTC columns. This information can be used to develop guidelines for the safe designs of such columns. It will also provide the basis for development of simple analysis methods so that complicated numerical analysis may be dispensed with in practical design procedure.

### 1.6 Scope and limitation of the study

The scope of the research study focused on the numerical investigation of axial loading response of CFDSSTC columns. In this paper, the behavior of concrete filled double skin steel tubular circular (CFDSSTC) column under axial compression load was studied. The parameters used in this study were the hollowness ratio ( 0, 0.25, 0.5, 0.75,1), length of the column (0.6m, 1m, 1.5m, 2m, 2.5m, 3m, 3.5m, 4m), thickness of the outer steel tube (2mm, 2.5mm, 3mm, 3.5mm, 4mm), and thickness of the inner steel tube (2mm, 2.5mm, 3mm, 3.5mm, 4mm) in order to determine the axial load carrying capacity and the axial deformation of different models. The response of the columns for both short and long columns was studied. It was also assumed that the columns consist of compact mild steel hollow sections and filled with self-compacting concrete with standard compressive strength, which commonly used in industry. Loads were limited to

concentric axial load. The most important works to be done are outlined in the research methodology.

The study was limited by the following

- ✓ Only circular columns were studied.
- ✓ Due to budget and laboratory constraints, experimental work was not conducted.
- ✓ In this study only C25 concrete was used for the investigation of the load carrying capacity of all CFDSSTC columns

## CHAPTER TWO

### LITERATURE REVIEW

#### 2.1 General

The steel-concrete composite was a compression member, comprising either a concrete encased hot-rolled or cold formed steel section or a concrete filled tubular section of hot-rolled or cold-formed steel and is generally used as a load bearing member in a composite framed structure. The combination is done in such fashions that, advantage of both the materials are utilized effectively [4].

In paper [5] Composite action between the various structural elements in a structural always exists when they are continuous. Depending on the size the building, certain simplifications may be made to approximate their interaction, as isolated structural components, in a conservative manner. The use of higher strength materials and composite action are important factors in making entire systems work economically. Tall buildings require additional considerations such as slenderness, flexibility, and sensitivity to differential effects. Steel and concrete are the major materials used in composite systems. Although they have several dissimilar physical characteristics, it is possible to use them together, beneficially, in different ways. A number of systems have been developed in the last few decades which successfully combine steel and concrete.

As mentioned above, the combination of concrete and steel in the column structure was initially aimed towards achieving fire resistance. The steel concrete composite action which occurred owing to the bonding between concrete and steel materials was later found to have an effect on the structures strength. As a result, an extensive study concerning the assessment of the composite action in the columns was conducted.

Self-compacting concrete (SCC) is highly workable concrete that can flow through densely reinforced and complex structural elements under its own weight and adequately fill all voids without segregation, excessive air migration (air-popping), or other separation of materials, and without the need for vibration or other mechanical consolidation.

The mix composition of SCC are same as those used in traditional vibrated concrete, but additional care is needed in the initial selection of materials used for producing SCC. The materials are included powder materials (cement, fly ash, silica fume, ground blast furnace slag, limestone and pigments), aggregates (fine and coarse aggregate) and water.

The paper in [6] reported that the compressive strength of SCC depends on (water/(cement + powder)) ratio, degree of compacting, type of cement and aggregate, age of aggregate and other factors, the compressive strength increases with the decrease of (w/c+p) material ratio. In rich SCC mixes increasing the maximum size of aggregate lead to decrease the compressive strength. In recent few decades, finite element (FE) technique is becoming increasingly popular for modeling CFST columns. FE analysis allows the direct modeling of the composite action between the steel and concrete components, and different factors, such as local and global imperfections, residual stresses and boundary conditions, can be considered more precisely. The prediction accuracy of a FE model, however, is greatly affected by the input parameters, especially by the selection of a suitable concrete model.

Recently, the concrete filled double skin steel tubular circular tube section was introduced in the hollow tube family. Since it is the newest steel section, only a handful of investigations on the application of this column structure had been undertaken. However, most of the researchers conducted so far have involved such type of composite columns. Therefore, it is considered that further investigations and experimental data are needed in order to develop a better understanding of the CFDSSTC columns particularly on slender columns behavior.

## 2.2 Types of concrete filled steel columns

Different types of composite columns are generally in use which can be categorized as steel section encased in concrete and steel section in-filled with concrete. Concrete-encased composite columns have structural steel components that could be either one or more rolled steel sections. In addition to supporting a proportion of the load acting on the column, the concrete encasement enhances the behavior of the structural core by stiffening it, and so makes it more effective against both local and overall buckling.

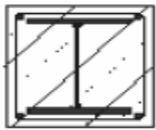
A concrete filled steel tubular (CFST) structure consists of steel hollow tube of square, rectangular or circular cross-section filled with either plain concrete or concrete with longitudinal and transverse reinforcement. In these paper concrete-filled steel tubes without reinforcement bars are covered.

Following are the various types of CFST columns:

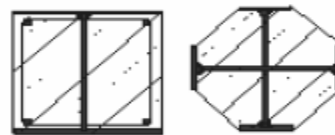
- ✓ composite column systems
- ✓ reinforced composite column systems
- ✓ concrete-filled double skin tubes(CFDST)

- ✓ Reinforced concrete-filled double skin tubes (CFDST)
- ✓ Concrete-encased CFST columns
- ✓ Stiffened CFST columns

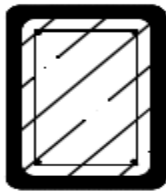
In paper [7] Concrete filled steel tubular (CFST) members comprise of a steel hollow section of circular or rectangular shape filled with plain or reinforced concrete. They exploit the advantage of both steel and concrete. They are extensively used in high-rise and multistory buildings as columns and beam-columns, and as beams in low-rise industrial buildings where a strong and efficient structural system is required.



a) Fully encased composite column



b) Partially encased composite columns



c) Concrete-filled column with reinforcement



d) Concrete-filled tube without reinforcement



e) Concrete-filled tube with structural steel sections

Figure 2.1: Typical cross section of composite columns ( Ermiyas Ketema, A.A University thesis).

### 2.3 Behavior of CFT column

A column is a structural element which primarily loads in compression along its length. It can be either subjected to axial compression loads or combined with eccentric load or bending moment. The failure of short compression columns is the result of compression axial loads, whereas in the case of longer columns, compression members are affected by the strength and stiffness of the material, as well as the geometry of the members.

The outer and inner steel hollow section is known to be a very efficient structure in terms of resisting compression axial loads, and has been widely used in the case of framed structures in industrial buildings.

In spite of this, as the development in the steel industry has moved forward, there have been many approaches to fire protection offered for exposed steel columns. Furthermore, as the construction technology advances, concrete infill in the hollow section are not only expected to increase the capacity of the structure, but also to increase its overall fire resistance.

In [8] found that there are several factors which may have a considerable effect on the ultimate strength of CFT columns, such as slenderness ratio, thickness, cross-section shape, and the mechanical properties of steel and concrete.

The paper in [9] reported that the compression axially loaded long CFT members can fail in two ways: in terms of slenderness and material properties. In the case of short columns, mechanical properties play a significant role in their behavior. The failure state is attained when the steel tube reaches the limit state of yielding and concrete crushing. On the other hand, stability will essentially govern the ultimate load capacity of slender CFT columns, where the members are more likely to fail as a result of buckling and second-order effects becoming more critical.

The shape of the column has also contributed to the strength and behavior of CFT column. Comparing the open section and the hollow tube, the latter is considered to be the most efficient shape for the compression member owing to its material distribution, which is further away from the center of the cross-section. However, the disadvantage remains that the structure member is difficult in terms of connection.

Nowadays, there are many types of hollow steel tubes available in the market. Amongst them, the circular hollow section is evidently the most efficient for compression members. The effect of the cross-section shape and thickness on the ultimate axial strength of CFT columns has been acknowledged from research carried out by [10] from the study, it was concluding that the short

axially loaded circular CFT columns have an elastic-perfectly plastic behavior, and also offer more post-yield axial ductility when compared with the square or rectangular CFT column. This exhibited by the significant strain hardening behavior of the circular column, whilst various post-yield behavior depending on the tube wall thickness of the tube column, were exhibited in the case of square and rectangular tubes.

#### 2.4 CFDSSTC column under axial compression loads

Axial force is the major force applied to columns in tall buildings. The benefit of using concrete filled columns is to enhance the load carrying capacity of columns. Many experiments were conducted on concrete filled columns subjected to axial loads. The ultimate loads of short columns with stocky tubular sections are considerably larger than the nominal axial load capacities. The reason for this increase in the ultimate load is attributed to the strain hardening effect of steel tubes and confinement effect of concrete [11].

In [12] found that, the measured axial load carrying capacities of concrete filled steel tubes was greater than the nominal capacity, which was defined as the sum of the compressive strength of the unconfined concrete and steel. This was related mainly to triaxial containment of the concrete and the strain hardening of the steel.

There are a number of researches and articles which address the analysis of concrete filled double skin steel tubular circular column under axial loads. One of the papers in [13] reported that, when the concrete filled double skin steel tubular circular (CFDSSTC) column member is axially compressed, the three components, inner tube, outer tubes, and the concrete are supposed to be subjected to the same axial strain. The axial load sustained at this strain is the sum of the forces acting on the three components.

$$N = A_c f_c + A_{it} f_{it} + A_{ot} f_{ot} \text{-----} (1)$$

Where:

$A_c$  = cross sectional area of concrete.

$A_{it}$  = cross sectional area of inner steel tube.

$A_{ot}$  = cross sectional areas of outer tube.

$f_{it}$  = axial stress of the inner steel tube.

$f_{ot}$  = axial stress of the outer tube.



In paper [14], a set of CFDSSTC columns with inner and outer tubes made of steel and have circular shape have been prepared according to the experimental program to be tested, figure 2.2 shows a schematic view of the CFDSSTC columns specimens.

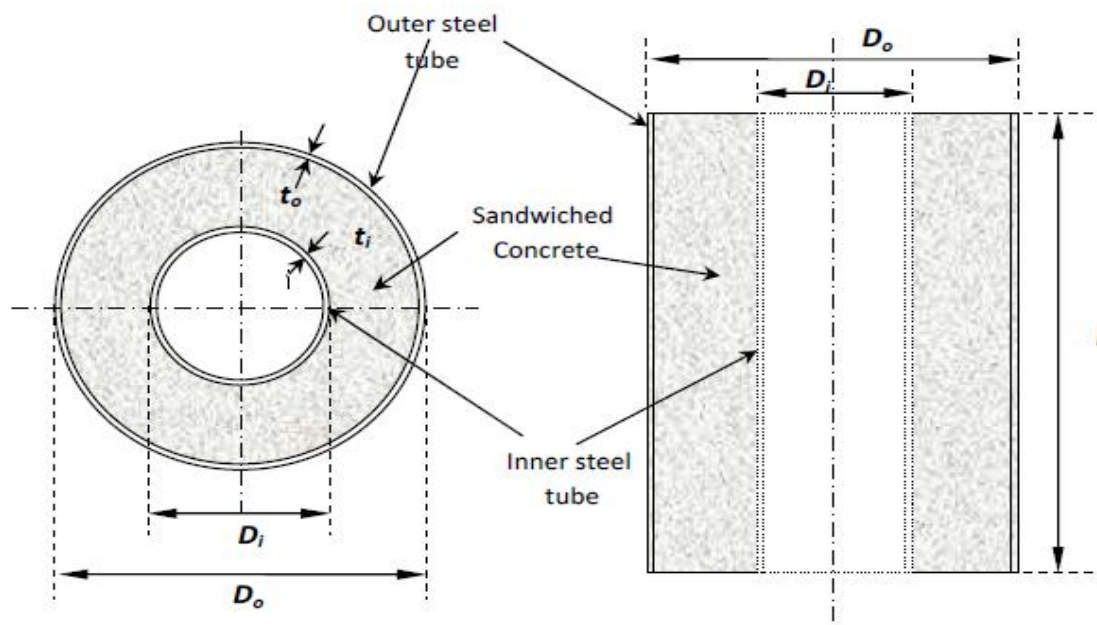


Figure 2.2: CFDSSTC columns details [14], a) cross section, b) longitudinal section.

## 2.5 Advantage and disadvantage of CFDSSTC columns

There are many relative advantages of using CFDSSTC columns rather than using the other columns types. These are:

- ✓ Concrete and steel are completely compatible and complementary to each other as they have almost same thermal expansion and they have an ideal combination of strengths with the concrete efficient in compression and the steel in tension.
- ✓ Composite construction, particularly that uses CFTs, allows rapid construction as there is no need for form work construction. In addition, waiting for curing time of concrete is not necessary as construction of upper story can proceed before curing of concrete in the lower story.
- ✓ Steel is positioned at the furthest location of the cross-section to produce the maximum flexural moment due to the maximum level arm. Whereas, in reinforced concrete the possible position of reinforcement is within the cross-section allowing for cover requirement.

- ✓ The steel section can replace the function of longitudinal reinforcement and transverse confinement by carrying longitudinal and transverse load and at the same time providing confinement (even in a better way). As a result, provision of longitudinal and transverse reinforcement may be eliminated.
- ✓ continuous confinement provided by the steel tubes prevent excessive spalling of concrete and on the other hand, the concrete filled inside the steel tubes prohibits local inward buckling of the steel tube wall, consequently providing efficient system.
- ✓ Suitable for high rise structures or structures that need wider free space because of their high strength and flexibility.
- ✓ The ductility requirement for earthquake resistant design is easily achieved by using CFT than the common reinforced concrete column or encased composite column.
- ✓ Vibrations caused by earthquakes and winds can be reduced due to its higher rigidity than that of steel columns.
- ✓ Column sections in the composite structural system can be reduced because of its high strength. It is also possible to keep the same column dimensions over several story of a building, which provides both functional and architectural advantages.
- ✓ Due to interactions of three components of CFDSST (outer steel, concrete and inner steel pipe) column they have high flexural stiffness, avoiding instability under external pressure, results in a good position stability, increased section modulus, improved overall stability, better seismic strengthening, better coupled with a circular steel columns, light weight, and performance characteristics of a good attenuation [15].

Disadvantages of CFST columns are:

- ✓ Under uni-axial compression, steel shares a larger part of the external load than concrete per same cross-section area because of higher stiffness under composite action.
- ✓ Under flexural, the central concrete, which is closed to the neutral axis, has insignificant contribution to the flexural strength.
- ✓ Under torsion, the central concrete has insignificant contribution to the torsion strength.
- ✓ The initial elastic dilation of concrete under compression is small and thus the confining pressure provided by the steel tube to concrete is relatively low during elastic stage. It can only develop more rapidly until micro-cracking of concrete have been formed.
- ✓ Composite construction need to provide corrosion and fire resistant coatings [16].

## 2.6 Structural behaviors of CFDSSTC columns

### 2.6.1 Effect of Confinement

Concrete filled steel tubular circular (CFSTC) columns are found to be possessing improved structural properties compared to conventional columns due to the composite action of steel tube and core concrete. CFST columns are considered to be efficient in providing a significant amount of confinement while this effect is not remarkable in the rectangular sections or square sections. An increase in strength takes place due to the increases in compressive strength of the in-filled concrete that is particularly restrained laterally by the existence the surrounding steel tube. This rise in concrete strength offsets the reduction in the vertical compression yield strength of steel due to the confinement required to constrain the concrete. The confinement effect does not occur in concrete filled rectangular hollow sections uniformly, as the hoop tension induced along the rectangular tube walls is not constant as reported by many researchers. In the circular sections of in-filled concrete the effect of confinement is brought down by the application of bending moments or columns subjected to eccentric load. This is because the mean compressive strain in the concrete (and the combined lateral expansion) is reduced.

It is also reduces with the increase in slenderness ratio of the columns, since, lateral deflection before failure increases the confinement which may occur for columns where in-filled concrete is crushed in advance to local buckling of steel and this would generally hold for columns, where the plate slenderness limit is notably small.

The confinement effect introduced by the steel tube in the concrete core is an important aspect of the structural behavior of CFDSST columns. In paper [17] discuss the confinement mechanism in the early stage of loading is minimal and can be neglected, since the poisons coefficient of the concrete is smaller than the steel poisons coefficient. Therefore, the steel tube expands faster than the concrete core in the radial direction and the steel tube does not restrain the concrete core. At this point no separation does exist between the steel and the adjacent concrete. However, when the applied load reaches the uniaxial strength of concrete, the concrete micro cracking initiates and propagates. The concrete lateral expansion reaches its maximum, mobilizing the steel tube and efficiently confining the concrete core. The ultimate capacity of the CFT columns is therefore higher than the sum of the resistance of their components. The radial stress introduced by the steel tube on concrete is responsible for the additional resistance of the

concentrically loaded CFT columns where the concrete core is subjected to a triaxial stress state and the steel tube is under a biaxial stress state.

The sections shape effect on confinement was investigated in paper [18], as has been ascertained from the study, the confinement is found to be superior in circular and octagonal CFT columns, but not in CFT columns with a square steel section. This is owing to the uniformed lateral pressure in the circular tube which confines the concrete core; in the case of the square section, however, higher confining pressure only occurs at the center and corner of the section compared to the other side.

In paper [19] stated that the confinement effect of concrete core results in triaxial state of stress of concrete core thereby avoids the inward buckling of steel tube and thus increasing the strength and stability of CFT columns. The failure load will be considerably larger than the sum of steel and concrete failure loads. The level of increase in the failure load of CFTs caused by the confining effect of the steel tube on concrete core is influenced by factors such as cross-sectional shape, length to diameter ratio, diameter to thickness ratio or thickness of steel tube, eccentricity of loading, concrete core strength and steel strength. And also investigate concrete under triaxial loads has a larger capacity and filling the tube with concrete must increase its ultimate strength and concluded that for concrete filled circular steel sections, axial strength of column increases due to confinement effect as concrete core is restrained laterally by the surrounding steel tube

The increase of concrete resistance from  $0.85f_{ck}$  to  $f_{ck}$  for concrete-filled hollow sections as compared with reinforced concrete and concrete encased columns is due to the effect of confinement (EBCS 2 1995, section 2.4).

In paper [20] states that on rectangular tube the tension hoop developed along the side of the tube was not constant, and therefore seems to be the reason as to why a confinement effect was not present except in the corner of the steel tube. In paper [21] suggested that confinement is considered to be more significant in the case of circular CFT columns rather than square CFT columns, where the column only shows a small increment in axial strength the confinement in the square section was found to be more effective than the rectangular section.

## 2.6.2 Axial buckling

Buckling is one of the structural behavior and an instability form which should be considered primarily for compression members, such as columns. Its presence obviously reduces the capacity of the structure. Eurocode 4 (EC4), for instance, has imposed some restrictions on the allowable diameter-to-thickness ratio,  $D/t$  in order to prevent local buckling from influencing structure capability as indicated in table 2.4a in BS EN 1994-1-1:2004.

### 2.6.2.1 Local buckling

There are two types of buckling: local buckling and overall buckling. Local buckling occurs when the thin steel elements are compressed in their planes. In paper [22] states that in order to fully utilize the steel strength, the failure mode should be prevented before the steel reaches its yield stress. In the case of thin walled steel tubes, the influence of local buckling is significant is significant to its strength. This type of failure is indicated by the growth of bulges, waves or ripples. In the case of CFT columns, the presence of concrete infill has an effect in prolonging the local buckling of the tube wall. In [23] the contribution of concrete core in delaying the occurrence of inward local buckling could insure that the steel would reach its longitudinal yield strength before buckling took place. The other advantage of having only outward mode failure mechanism is the prevention of significant decreases in the section modulus. This is owing to the fact that the distance between the top and bottom flanges of the steel increases rather than decreases (as without) the concrete core when local buckling occurred. The presence of local buckling is also known to affect the confinement is limited as the tube sections were prevented from providing a continuous restraint on the concrete for confinement. However, if the local buckling is inelastic, then the confinement of concrete can nevertheless develop.

Most researcher validated local buckling in the steel sections does not occur. To prevent premature local buckling, the width to thickness ratio of the steel sections in compression must satisfy the following limits:

- $\frac{d}{t} \leq 85\epsilon^2$  for concrete filled circular tubular sections, where  $\epsilon = \sqrt{\frac{250}{f_y}}$

The initiation of local buckling can be determined by examination of the contact force between the outer and inner steel tube and concrete core. The variation of internal force is similar to the

changes in confining pressure. The aspect ratio has a significant effect on the local buckling of steel tube.

The plastic resistance to compression of a concrete steel composite cross-section  $P_p$ , represents the maximum load that can be applied to a short column. For slender columns with low elastic critical load, overall buckling may be critical. In a typical buckling curve for an ideal column shown below (a), the horizontal line represents  $P_p$ , while the curve represents  $P_{cr}$ , which is a function of the column slenderness. These two curves limit the compressive resistance of ideal column.

For convenience, column strength curves are plotted in non dimensionalized form as shown in figure (b), the buckling resistance of a column may be expressed as a proportion  $F$  of the plastic resistance to compression,  $P_p$ , there by non-dimensionalizing the vertical axis of figure (a), where  $F$  is called the reduction factor. The horizontal axis may be non-dimensionalized.

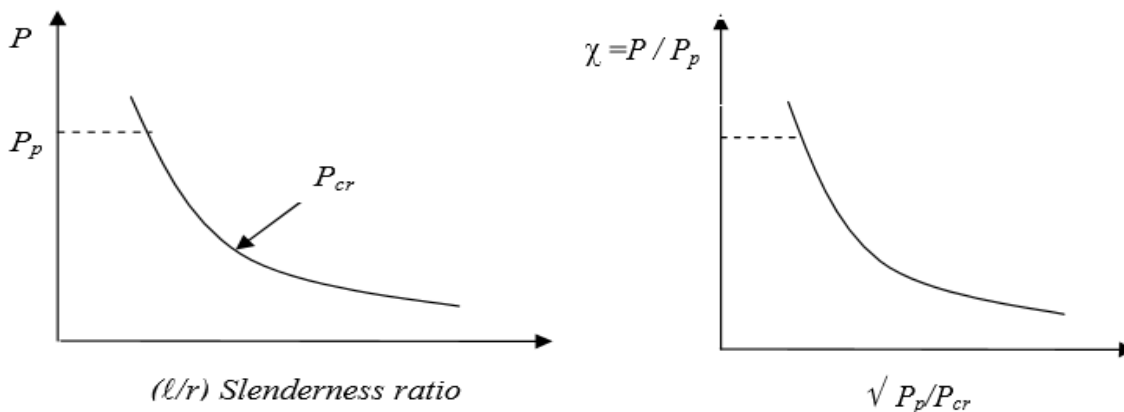


Figure 2.3: Idealized column buckling curve (a), non-dimensional column buckling curve (b).

### 2.6.2.2 Overall buckling

Overall buckling generally occurred in the case of long or slender columns. The failure is illustrated by sideways bending where, for the particularly columns, the global stability is more vulnerable, as the columns tend to fail owing to flexural buckling [24]. This failure occurs when the condition of a stable equilibrium between the internal and external forces in the structure is no longer possible. The behavior of these columns is influenced by the slenderness ratio, with the slenderness also contributing to the so-called second order effects.

### 2.6.3 Bond between concrete and steel

Bond develops either from adhesion between concrete and steel or from friction due to normal stress. Since adhesion is active mainly at the early stage of loading, it is assumed that bond between the concrete and the steel is mainly contributed by friction [25]. Friction develops between the concrete core and the steel tube due to the coefficient of friction and normal contact pressure, which is caused by lateral expansion of the concrete core when subjected to compressive loading. The magnitude of the friction force developed in CFDSST columns depends on the rigidity of the tube walls against pressure perpendicular to their plane.

The significance of bond strength of the composite section depends of the condition of load applications. When the load is applied at the column end only to the steel section or only to the concrete section, the load must be transferred over the contact surface from the concrete core to the steel tube or vice versa. For this transfer sufficient bond is necessary. Otherwise, the load will not be shared between the concrete and steel in proportion to their strength.

When the load is applied to the entire section, the contributions by the concrete core and steel tube to the total load carrying capacity are in proportion to strength and will be constant along the height of the column, and thus, bond will not affect the strength significantly.

In [26] Experiments when the load is applied to the steel section, the steel tube carried almost the whole load through the column and a higher coefficient of friction gave just a small increase in the load resistance. That is, transfer of load from steel to concrete is hardly achieved by the natural bond between concrete and steel. A better load transfer is observed when the load is applied to the concrete, although not sufficient to assume full composite strength.

It is the opinion of many researchers that at the initial stage, the applied load is resisted individually by the steel and concrete elements. That too, the steel sustains larger part of the loading, until yielding. At the early stages of increment of loads, the poisons ratio of concrete lies far below than that of the steel whereas, steel tube causes no confinement on the concrete. With the increase in the longitudinal strain beyond a particular stage, an increase in the poisons effect in the concrete attains, as a result of lateral expansion of the concrete. At this stage, the longitudinal and hoop stresses in the steel plate are becoming equal. Steel plate is bi-axially stressed and concrete being tri-axially stressed the expansion of the concrete takes place more than that of the steel. It is followed by the redistribution of load from concrete to outer steel mainly. At this stage, the steel shows hardening character [27].

The transmission length of the shear force should not be assumed to exceed twice the transverse dimension. If the bond is not sufficient to transfer the load within this length, it is necessary to provide the top region of the steel tube with mechanical shear connectors at the inside to ensure full composite action. Thus, effect of bond has to be considered for the design of connectors. For the purpose of calculation, the design shear strength due to bond for concrete-filled tube not be taken more than 0.4Mpa to take large value, it should be verified by tests [EBCS4-1995].

Experiments also indicate that bond strength is larger in circular versus rectangular CFTs, and that it decreases with an increase in the depth to steel thickness ratio [28].

In [29] the bond strength between the steel tube and core concrete in full scale concrete filled steel tubes. The parameters such as steel type (stainless steel and carbon steel), concrete type (normal and expansive concrete), age of concrete (28 days and 3 years) and interface type (normal interface, interface with shear studs and interface with an internal ring). The result show that the concrete filled stainless steel tubular column have lower bond strength compared with the concrete filled carbon steel tubular column. Meanwhile, the bond strength decreases remarkably with increasing concrete age.

#### **2.6.4 Roles of steel tubes in composite columns**

In paper [30], experiments test were studied to assess the behavior of six inner and outer steel tubes without concrete core. The length of all the stub columns was 400mm. the diameter of external tubes ( $D_o$ ) was varied from 114 to 165 mm and that of the inside tubes ( $D_i$ ) was varied from 48 to 102mm. the diameter to thickness ratio of the outer and inner tubes range from 19 to 57 and 17 to 33mm respectively. When an axial load was applied the axial load capacity increase as the thickness of both inner and outer tube increase.



Table 2.1: Axial load resisting performance of different outer and inner tube thickness [30].

Test	Location	Diameter(mm)	$N_T$ (KN)
1	Outer	114.5	927
2	Outer	114.6	719
3	Outer	114.4	560
4	Outer	114.2	454
5	Outer	165.1	674
6	Outer	165.3	553
7	Inner	48.4	228
8	Inner	101.8	414

### 2.6.5 Load transfer mechanisms

In paper [31] stated that the ultimate axial capacity of CFT columns is larger than the sum of uncoupled steel and concrete failure loads. The increase in the failure load is caused by the confining effect of steel tube on the concrete core. The structural behavior of CFTs is considerably affected by the difference between the Poisson's ratio of the steel tube and concrete core. In the initial stage of loading, the Poisson's ratio for the concrete is lower than that of the steel. Thus, the steel tube has no confining effect on the concrete core. As longitudinal strain increases, the lateral expansion of concrete core gradually becomes greater than expansion of steel tube. At this stage, the concrete core becomes triaxially stressed and steel tube biaxially stressed. The steel tube under a biaxially state of stress cannot sustain the normal yield stress, causing a transfer of load from tube to the core. In the first stage of loading the steel tube sustains most of the load until it yields (point A). at this point (A) there is a load transfer from the steel tube to the concrete core. The steel tube exhibits a gradual decrease in load sharing until the concrete reaches its maximum compressive strength (A to B). After this stage of loading (point B), there is a redistribution of load from concrete core to the steel tube. At this point (B) the steel exhibits a hardening behavior with almost the same slope as in the uniaxial stress-strain hardening relationship ( $E_t$ ). The maximum confined compressive stress of concrete core in circular columns is higher than square columns.

## 2.6.6 Columns load capacity

### 2.6.6.1 Axial compression

Resistance of a composite cross-section subject to different loading is discussed based on EBCS 4, 1995. The cross-sectional resistance of a composite column to axial compression is the aggregate of the plastic compression resistances of each of its constituent elements as follow:

$$N_{pl,Rd} = A_s * f_{yd} + A_c * f_{cd}$$

$$\text{where } f_{yd} = \frac{f_y}{\gamma_{m2}} \text{ and } f_{cd} = \frac{f_{ck}}{\gamma_c}$$

$A_s$  and  $A_c$  are respectively the cross-sectional areas of the profile and the concrete

$f_y$  and  $f_{ck}$  are characteristic steel and concrete strength in accordance with EBCS 3-1995 and EBCS 2-1995, respectively.

$\gamma_s$  and  $\gamma_c$  are partial safety factors for steel and concrete respectively.

$$\gamma_s = 1.10 \text{ and } \gamma_c = 1.5$$

For a concrete –filled circular hollow section, a further increase in concrete compressive resistance is caused by hoop stress in the steel section. This happens only if the hollow steel profile is sufficiently rigid to prevent most of the lateral expansion of the concrete under axial compression. This enhanced concrete strength may be used in design when the relative slenderness of the composite column does not exceed 0.5 and the greatest bending moment  $M_{max.sd}$  (calculated using first-order theory) does not exceed  $0.1N_{sd}$ , where  $d$  is the external diameter of the column and  $N_{sd}$  is the applied design compressive force. The plastic compression resistance of a concrete-filled circular section can then be calculated as:

$$N_{pl,Rd} = A_s * \eta_s * f_{yd} + A_c * f_{cd} [1 + \eta_c * \frac{t}{d} * f_{yd}]$$

In which  $t$  represents the wall thickness of the steel tube. The coefficient  $\eta_s$  and  $\eta_c$  are defined as follows for  $0 < e < \frac{d}{10}$ , where  $e = \frac{M_{max.sd}}{N_{sd}}$  is the effective eccentricity of the axial compressive force:

$$\eta_s = \eta_{so} + (1 - \eta_{so}) * (10 * \frac{e}{d})$$

$$\eta_c = \eta_{co} * (1 - 10 * \frac{e}{d})$$

$e > \frac{d}{10}$  It is necessary to use  $\eta_s=1.0$  and  $\eta_c=0$  in equations above the terms  $\eta_{so}$  and  $\eta_{co}$  are the values of  $\eta_s$  and  $\eta_c$  for zero eccentricity  $e$ . they are expressed as functions of the relative slenderness  $\lambda$  as follows:

$$\eta_{so} = 0.25(3 + 2\lambda) \leq 1$$

$$\eta_{co} = 4.9 - 18.5\lambda + 17\lambda^2 \geq 0$$

The presence of a bending moment  $M_{sd}$  has the effect of reducing the average compressive stress in the column at failure thus, reducing the favorable effect of hop compression on its resistance. The limits imposed on the value of  $\eta_s$  and  $\eta_c$ , and on  $\eta_{so}$  and  $\eta_{co}$ , represent the effects of eccentricity and slenderness respectively on the load-carrying capacity.

The elastic critical load  $N_{cr}$  of a composite column is calculated using the usual Euler buckling equation

$$N_{cr} = \frac{\pi^2 (EI)e}{l^2}$$

In which  $(EI)e$  is the bending stiffness of the composite section about the buckling axis considered, and  $l$  is the buckling length of the column. If the column forms part of a rigid frame this buckling length can conservatively be taken equal to the system length.

### 2.6.7 CFDSSTC columns modes of failure

The compressive axial strength of CFDSSTC columns is governed by a combination of yielding of the steel and crushing of the concrete. CFDSSTC columns with small length to depth ratios typically fail near their cross-section strength. Intermediate length or long (slender) CFDSSTC columns are governed by flexural instability, usually involving at least some crushing of the concrete and yielding of the steel prior to buckling.

Based on the mode of failure, composite columns are classified as stub or short columns which attain failure are generally governed by the yield strength  $f_y$  of the steel and characteristic strength  $f_{ck}$  of the concrete. Hence, the stocky columns are termed as material dependent.

Moreover, such short tubes in-filled with concrete are also liable to local buckling and this is very true for the application of thin walled tubes in construction.

Whereas the long or slender columns do fail by so called flexural buckling as that of steel columns. In such situation, the composite columns become unsteady and undergo buckling laterally with the buckling half wavelength being in the order of the length of the columns. Certain important structural considerations that shall be kept in mind when comparing basic behavior of composite columns, whether the type is enclosed columns or in filled concrete steel tubes are a) in-filled concrete tubes are like to be affected by local buckling of the steel skin which in many cases is very thin, b) lateral restraint is offered by the tube against the possible expansion of core concrete in compression. This ultimately improves overall strength of short columns, but it is irrelevant in slender columns, c) steel tube mitigates the ingress of moisture, which results in minimizing creep and shrinkage effects. Research on time dependent deformations of concrete filled tubes has proven to reduce creep and shrinkage response. Hollow sections in-filled with concrete have many benefits such as higher dial load carrying capacity and elimination of the need of formwork. In addition to all these, the concrete being in a confined state dissipates more energy and also leads to increased local buckling strength of the steel sections in general.

In [32] conducted an experimental behavior of circular concrete-filled steel tube columns. This paper presented on experimental study on behavior of circular in-filled steel tube (CFT) columns with self-compacted concrete (SCC) concentrically loaded in compression to failure. Seventeen specimens were tested to investigate the effects of concrete strength and different loading conditions on ultimate capacity and load-deformation behavior of columns. Specimens with entire section loaded experience a significant increase in ultimate capacity, but their residual after failure is almost constant. It was observed from the tests, that the failure mode of the hollow composite columns depends on slenderness ratio. When the slenderness ratio is very less, the column fails due to yielding of steel and crushing of concrete under direct compression. When slenderness ratio is more, the column fails by elastic buckling.

In paper [33] stated that the collapse of CFDSST columns is mainly due to the failure of the outer steel tube, which is caused by the combined axial compression and concrete expansion. The failure modes of outer steel tubes included the outward local buckling, while no failure was found in the inner steel tube. The cross sectional area of the confined concrete by the outer and

inner steel tubes has the most significant effect on the ultimate axial load capacity and corresponding axial shortening of CFDSST columns. There is a linear relationship between the outer steel tube thickness and the ultimate axial capacity of CFDSST, where an improved of about 8% was obtained when the thickness changed from 2mm to 4.5mm. The axial strength decrease with the increase of hollowness ratio, this degradation in strength is almost linear when hollowness ratio changed from 0.381 to 0.714, where about 20% lose in strength occurred.

In paper (34) discusses concrete have higher compressive strength and steel have higher tensile strength. In CFDSSTC column is a merging of the property steel and concrete. It can be seen that both inward and outward buckling failure is found in the steel tube, and shear failure is happen for the plain concrete stub column. For the concrete-filled steel tube, only local buckling is found in the tube, and the inner concrete fails acts like a ductile material.

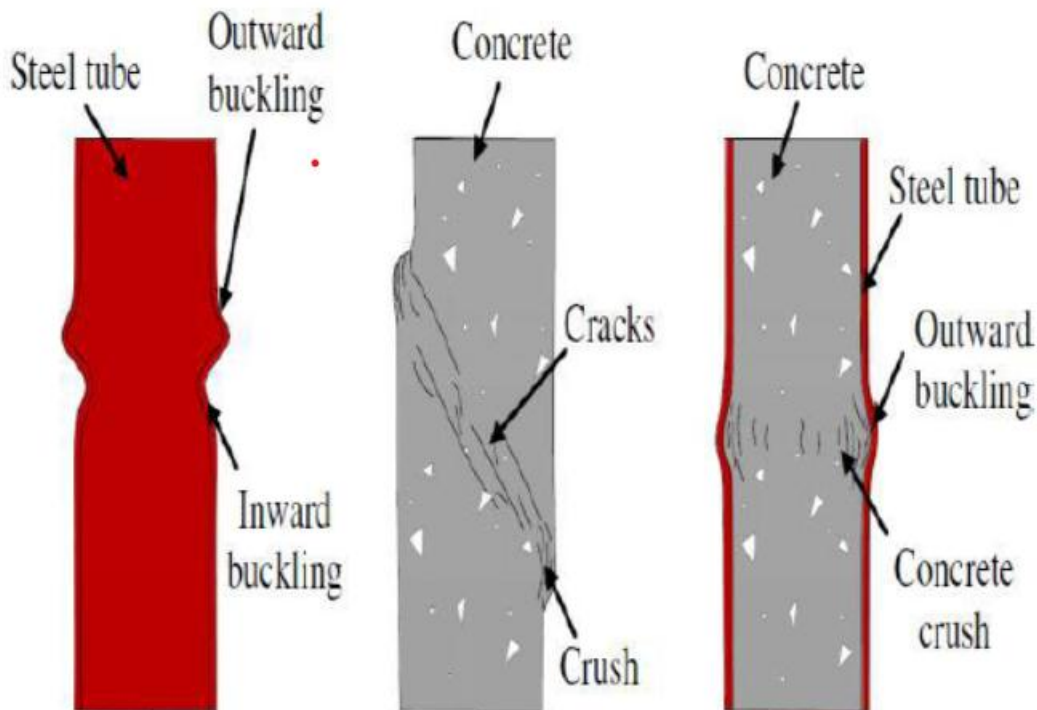


Figure 2.4: Schematic failure modes of hollow steel tube, concrete and CFST stub columns [34].

In paper [35] double skinned columns fail in the same pattern of overall buckling and local buckling of outer steel plate in compression flange in the vicinity of mid height leads the failure. It was found that because of the infill of concrete, the tested beam-columns behaved in a relatively ductile manner and testing proceeded in a smooth and controlled way. The enhanced structural behavior of the composite specimens can be explained in terms of “composite action”

between the steel tubes and the filled SCC concrete. CFT columns carry almost similar load but the failure is sharp and brittle as in a RCC column.

### 2.6.8 Buckling resistance

A composite column has sufficient resistance to buckling if, for each of the planes of buckling, the design axial loading  $N_{sd}$  satisfies the inequality:

$$N_{sd} \leq \chi * N_{pl,Rd}$$

In which the value of  $\chi$ , the strength reduction factor in the plane of buckling considered, is a function of the relative slenderness  $\lambda$  and the appropriate buckling curve. The buckling curves which apply to composite concrete filled columns is “curve a” which is given in [EBCS 3-1995]. The plastic compression resistance of a composite cross-section represents the maximum loads that can be applied to concrete filled double-skin steel tubular columns. The concrete filled circular tubular sections exhibits enhanced resistance due to the tri-axial confinement effects. Fully or partially concrete encased steel sections and concrete filled rectangular tubular section do not achieve such enhancement.

For composite columns using circular tubular sections, there is an increased resistance of concrete due to the confining effect of the circular tubular section. However, this effect on the resistance enhancement of concrete is significant only in stocky columns. In general, the resistance of a concrete filled circular tubular section of compression may increase by 15% under axial load only when the effects of tri-axial confinement are considered.

### 2.6.9 Stress-strain relationship for concrete core and steel tube

In paper [36] states that Circular and square CFT columns exhibits different pattern of cross-section stress distribution in concrete core. In the case of square columns, the cross-sectional stress distribution is not uniform. The center and the corners of square section go under a higher confining pressure than the side. In case of circular columns, the axial and lateral stress distribution at the cross section is radially uniform. An equivalent axial stress is defined which is obtained by dividing the total concrete core axial load by the cross-sectional area of concrete core. It is well know that confined concrete exhibits higher compressive strength and larger ductility than unconfined concrete.

## CHAPTER THREE

### RESEARCH METHODOLOGY

#### 3.1 General

In this paper, a total of 23 models were created and analyzed in ABAQUS software to determine the axial capacity and failure modes of concrete filled double-skin steel tubular circular columns. The top and bottom surface of the concrete-filled steel tubular circular columns were fixed against all degrees of freedom except for the displacement at the loaded end, which is the top surface, in the direction of the applied load. This was done using remote displacement support for the top surface and fixed support for the bottom surface. In this section of the report; sample detailing, the study variables, non-linear Finite Element modeling and analysis steps of the selected columns were discussed in detail.

#### 3.2 Sample Detailing

In order to study the behavior of concrete filled double skin steel tubular circular (CFDSSTC) columns in-filled with self-compacting concrete (SCC) under compression, the hollowness ratio ( $\chi$ ), length of the column, the thickness of the outer and inner steel tube were the parameters investigated throughout this study. Each column was analyzed under axial compression loading which marked as (CFST). Table 3.1 show detail of the analyzing program of CFDSSTC specimen's.

Table 3.1: Analyzing program and CFDSSTC specimen's details.

Specimen no	Column designation	Do (mm)	to (mm)	Di (mm)	ti (mm)	$\chi$	L (mm)
1	CFST-1	114	4.5	40	3.3	-	600
2	CFST-2	114	4	0	0	0	1000
3	CFST-3	114	4	26.5	3	0.25	1000
4	CFST-4	114	4	53	3	0.5	1000
5	CFST-5	114	4	79.5	3	0.75	1000
6	CFST-6	114	4	-	-	1	1000
7	CFST-7	114	4	45	2	-	1000
8	CFST-8	114	4	45	2.5	-	1000
9	CFST-9	114	4	45	3	-	1000

10	CFST-10	114	4	45	3.5	-	1000
11	CFST-11	114	4	45	4	-	1000
12	CFST-12	114	2	45	3	-	1000
13	CFST-13	114.5	2.5	45	3	-	1000
14	CFST-14	115	3	45	3	-	1000
15	CFST-15	115.5	3.5	45	3	-	1000
16	CFST-16	116	4	45	3	-	1000
17	CFST-17	152	3	76	2	-	1000
18	CFST-18	152	3	76	2	-	1500
19	CFST-19	152	3	76	2	-	2000
20	CFST-20	152	3	76	2	-	2500
21	CFST-21	152	3	76	2	-	3000
22	CFST-22	152	3	76	2	-	3500
23	CFST-23	152	3	76	2	-	4000

Where:

$$\chi = \frac{D_i}{D_o - 2t_o}$$

$D_o$ : diameter of the outer steel tube

$t_o$  : thickness of the outer steel tube

$D_i$ : diameter of inner steel tube

$t_i$ : thickness of inner steel tube

$L$ : length of the steel tube and  $\chi$ : hollowness ratio



### 3.3 Non-linear Finite element analysis

The finite element method is a technique for approximating the governing differential equation for a continuous system with a set of algebraic equations relating a finite number of variables. These methods are popular because they can be easily programmed to solve FE techniques problems.

The finite element method is useful for the understanding of the behavior of concrete filled double skin steel tubular circular columns under axial compression loads. Experimental tests are needed to provide input data to the model and for the purpose of verification of simulation results. When the model has been validated it can be used for parametric studies to investigate the influence of various parameters.

The analysis of this study presented a nonlinear three-dimensional finite element modeling of circular tubular steel section filled with concrete for the investigation of the behavior of axially loaded composite concrete filled steel tubular circular columns strengthened with steel tube as external and internal confinement. The analysis was done using ABAQUS version 6.14 to build a finite element model for concrete filled double-skin steel tubular circular columns. The modeling and analysis procedure was described as shown below.

Note: all the specimens were modeled and analyzed after the FE software was validated for the specific case of this research.

#### 3.3.1 Parts (geometry) modeling

##### a) plain concrete columns

Plain concrete column parts were modeled on a 3D modeling space as deformable type with solid and extrusion base feature.

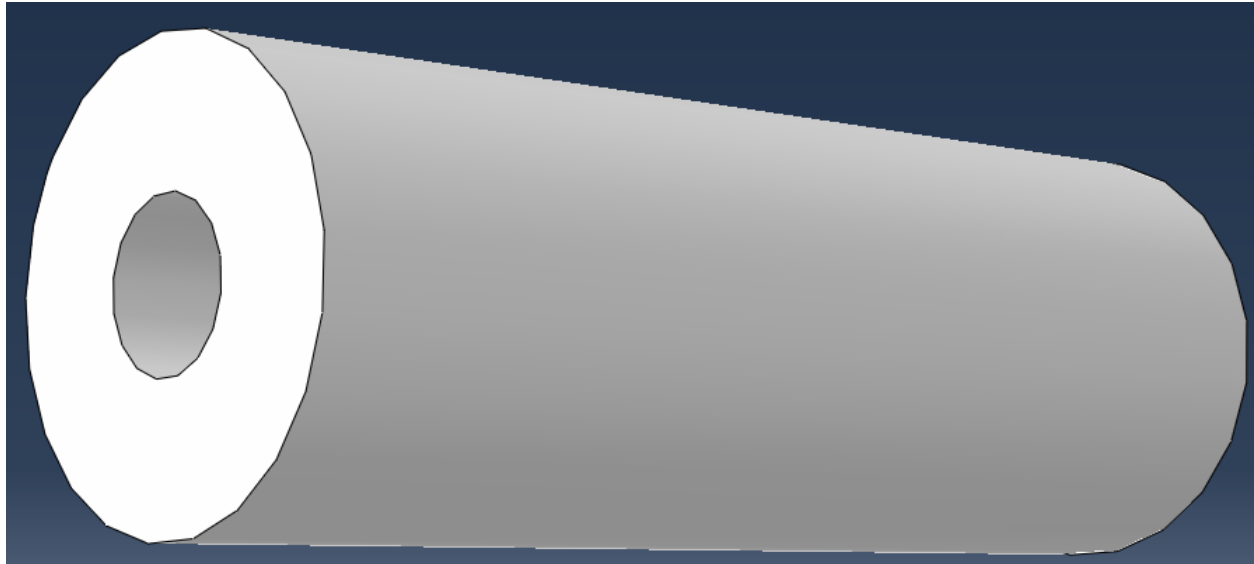


Figure 3.1: Plain concrete part for the first column.

b) steel columns

Steel column parts were modeled the same procedure as plain concrete columns. The steel part for the first column is shown in figure 3.2.

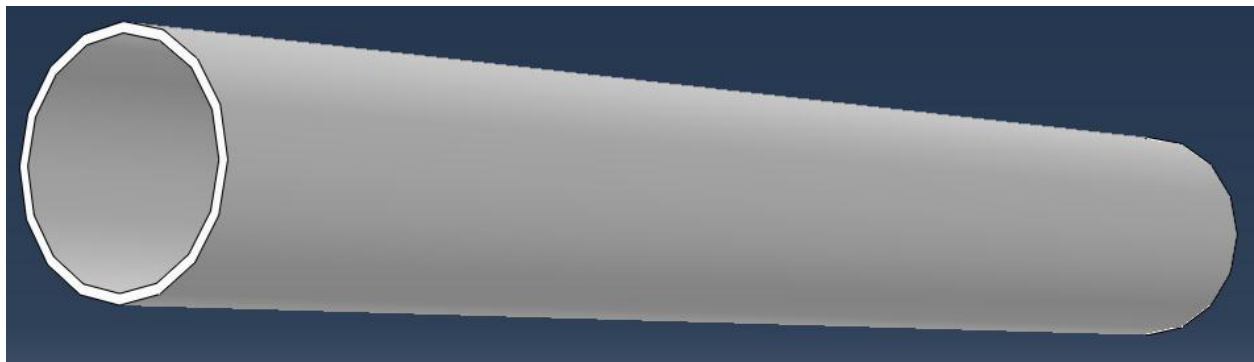


Figure 3.2: Steel column part for the first column.

c) loading steel plates

Thick Steel plates were used at the top and bottom end of the columns. They were modeled on 3D modeling space as discrete rigid type with shell and planar base feature. Since they are not study variable, they were kept similar for all columns.

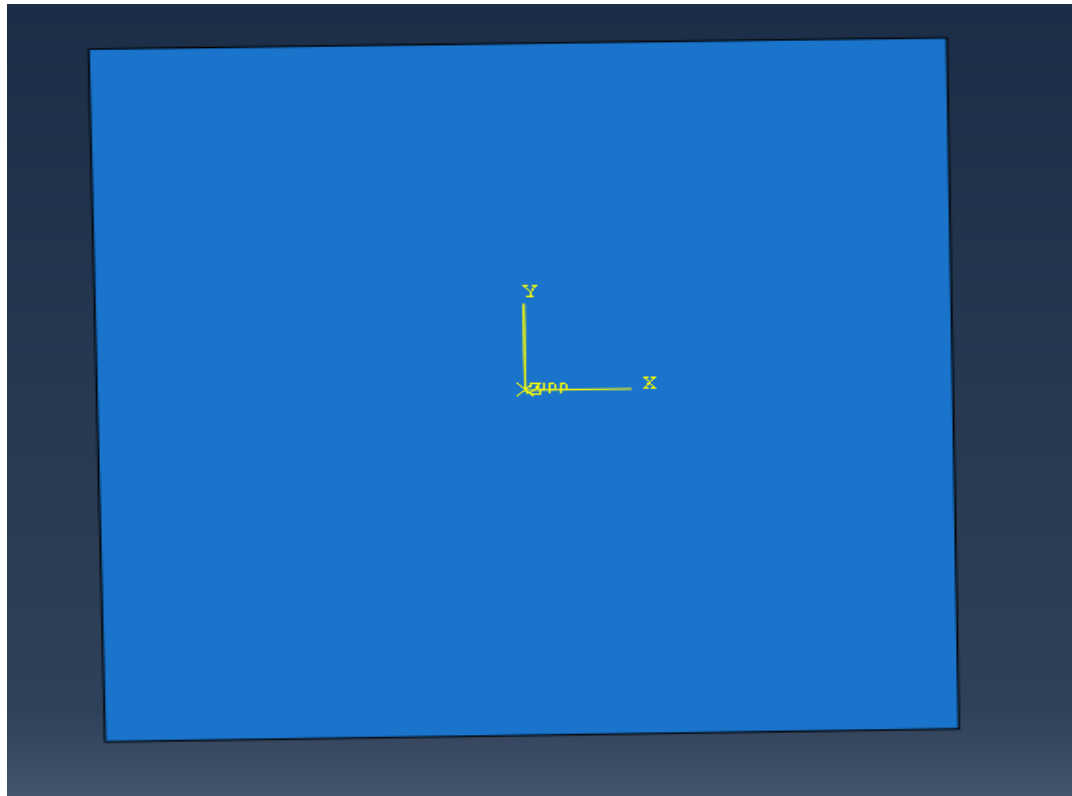


Figure 3.3: Loading steel plate part for the first column.

### 3.3.2 Part assembly and their interaction

After material properties, profiles and sections were created and assigned for the parts; instances were created for all parts and assembled to their relative position. Dependent instance was used for all parts.

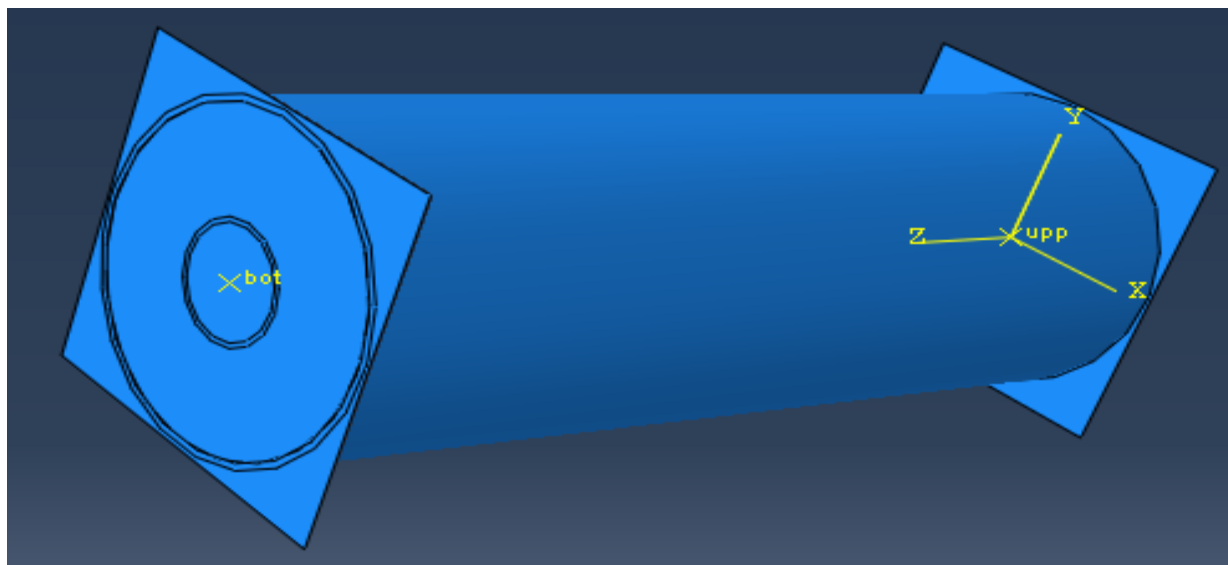


Figure 3.4: Assembled CFDSSTC column using ABAQUS for the first column.

The outer steel tube, inner steel tube and concrete core composite must behave as single member and not merely as a combination of three different materials. This makes the simulation of composite action between concrete, inner and outer steel tube the single most important factor guiding the behavior of the composite member. A General contact was used for the interaction simulation of the outer and inner steel tube with concrete. A contact surface pair comprised of the inner surface of the outer steel tube with outer face of concrete and outer surface of inner steel tube with inner face of the concrete core can be defined. “Hard contact” in the normal direction and a coulomb friction model in the tangential directions can be specified for the interface, which allows the separation of the interface in tension and no penetration of that in compression. For CFDSSTC columns, there is little or no slip between the steel tube and concrete since they are loaded simultaneously. For this reason, the columns behavior is not sensitive to the selection of friction coefficient between steel and concrete. Hence, a friction coefficient of 0.3 was used in the analysis.

The contact surfaces can model infinitesimal sliding and friction between the concrete core and interior and exterior steel tube, in which either contact or separate are allowed but not to penetrate each other. For the region between column end and steel plate, tie constraint was used by taking column surface as a master and plate surface as slave. This constraint enables both column and steel plate to act as one body. The final constraint which was used in the modeling was the rigid body constraint. This constraint makes the steel plate to act as discrete rigid and prevents deformation due to applied loading on its surface.

### 3.3.3 Materials modeling of steel

In paper [37] the bilinear kinematic hardening model as shown in figure 3.5, was used to simulate the stress-strain curve of steel and assumed to be an elastic-perfectly plastic material. The bilinear model requires the yield stress ( $f_y$ ) and the hardening modulus of the steel ( $E_s$ ), the constitutive law for steel behavior is:

$$\sigma_s = E_s \varepsilon'_s \quad \dots \quad \varepsilon_s \leq \varepsilon_y$$

$$\sigma_s = f_y + E'_s \varepsilon'_s \quad \dots \quad \varepsilon_s > \varepsilon_y$$

Where,  $\sigma_s$  is the steel stress,  $\varepsilon_s$  is the steel strain,  $E_s$  is the elastic modulus of steel,  $E'_s$  is the tangent modulus of steel after yielding,  $E'_s=0.01E_s$ ,  $f_y$  and  $\varepsilon_y$  are the yielding stress and strain of steel, respectively.

Statistical analysis indicates that high strength steel exhibits less strain hardening than normal strength steel. A  $\sigma - \varepsilon$  model was proposed by many researcher for structural steel with a validity range of  $f_y$  from 200Mpa to 800Mpa. This model was used to simulate the steel material in circular CFDSST columns.

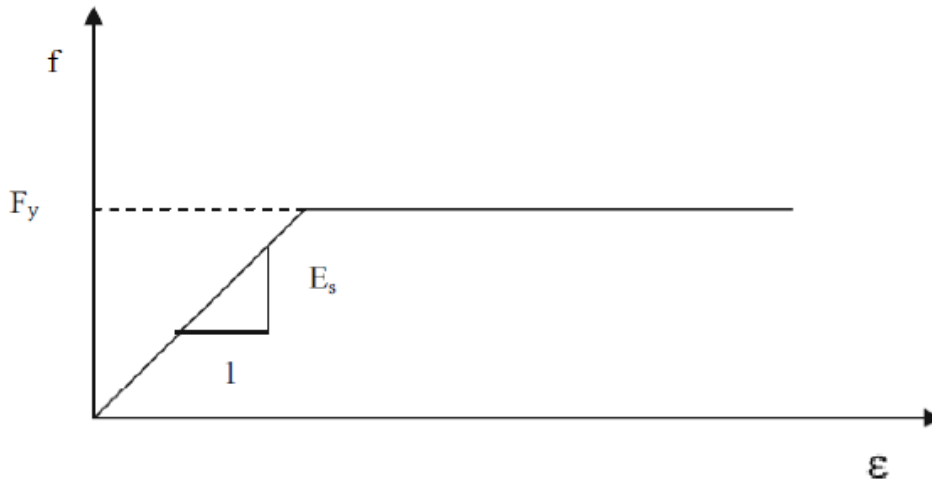


Figure 3.5: Elastic perfectly plastic model for steel tube [37].

The parameters which were used in this model that was input for the ABAQUS 6.14 were tabulated in table 3.2.

Table 1.2: Properties of steel.

Density	7850Kg/m <sup>3</sup>
Modulus of elasticity	200Gpa
Poisons ratio	0.3
Yield stress ( $f_y$ ) for outer steel	375Mpa
Yield stress ( $f_y$ ) for inner steel	250Mpa

### 3.3.4 Material modeling of concrete

For CFDSSTC columns under axial compression, the concrete core expands laterally and is confined by the outer and inner steel tube. This confinement is passive in nature, and can increase the strength and ductility of concrete. This mechanism is well understood and is often referred to as “composite action” between the steel tube and concrete in paper [38] state that the confined concrete is in a triaxial stress state and the steel is in a biaxial state after interaction between the concrete and steel occurs.

In paper [39] States that concrete exhibits nonlinear stress-strain response mainly because of micro-cracking. Cracks are oriented as the stress field and generate the failure modes. In tension, failure localized in a narrow band, stress-strain behavior is characterized by sudden softening accompanied with reduction in the unloading stiffness.

The equivalent uniaxial stress-strain curves for both confined and unconfined concrete are as shown in figure below, where  $f_c'$  is the unconfined concrete cylinder compressive strength, which is equal to  $0.8 (f_{cu})$ , and  $\epsilon_c'$  is the unconfined strain ( $\epsilon_c'$ ) is taken as 0.003. The confined concrete compressive strength ( $f_{cc}'$ ) and the corresponding confined strain ( $\epsilon_{cc}'$ ) can be determined from the eqs below.

$$f_{cc}' = f_c' + k_1 f_l \dots \dots \dots (1)$$

$$\epsilon_{cc}' = \epsilon_c' (1 + k_2 * f_l / (f_c')) \dots \dots \dots (2)$$

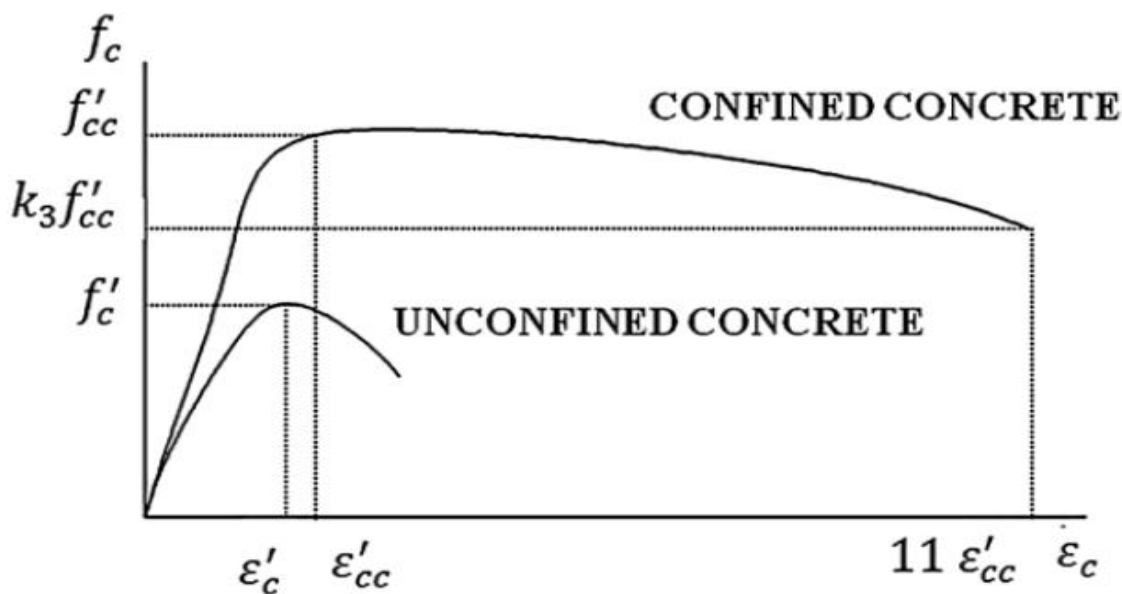


Figure 3.6: Uniaxial stress-strain curves for confined and unconfined concrete.

Self-compacting concrete (SCC) is highly workable concrete that can flow through densely reinforced and complex structural elements under its own weight and adequately fill all voids without segregation, excessive bleeding, and excessive air migration (air-popping), or other separation of materials, and without the need for vibration or other mechanical consolidation. The mix composition of SCC are same as those used in traditional vibrated concrete, but

additional care is needed in the initial selection of materials used for producing SCC. For concrete, ABAQUS requires an input data for material properties, which are elastic modulus ( $E_c$ ), ultimate uniaxial compressive strength ( $f_c'$ ), and ultimate uniaxial tensile strength, poisson's ratio ( $\nu$ ). The characteristic's cube strengths of concrete ( $f_{ck}$ )<sub>cu</sub>, is measured at 28 days.

a) concrete damage plasticity model

The concrete damaged plasticity model available in ABAQUS was used. Since this paper only deals with columns under monotonic loading, damage variables were not defined. Therefore, concrete nonlinearity was modeled as plasticity only. In this model, key material parameters to be determined include the ratio of the second stress invariant on the tensile meridian to that on the compressive meridian ( $k_c$ ), dilation angle ( $\psi$ ), and strain hardening/softening rule. Other parameters include the modulus of elasticity ( $E_c$ ), flow potential eccentricity ( $e$ ), ratio of the compressive strength under biaxial loading to uniaxial compressive strength ( $f_{bo}/f_c'$ ), viscosity parameter and tensile behavior of concrete. For the FE model presented by [34], constant values of  $20^\circ$  up to  $30^\circ$ , 0.1, 1.16, and  $2/3$  were used for  $\psi$ ,  $e$ ,  $k_c$ , and  $f_{bo}/f_c'$ , respectively. Default values of 0.1 and 0 were used for the flow potential eccentricity and viscosity parameter, respectively. These two parameters have no significant influence on the prediction accuracy. Although CFDSSTC columns are not sensitive to tensile behavior of concrete when subjected to axial compression, tension stiffening need to be defined in ABAQUS. The parameters which were used in ABAQUS software was tabulated in table 3.3.

Table 3.3: Properties of concrete.

Density	2400Kg/m <sup>3</sup>
Modulus of elasticity	31.476Gpa
Poisons ratio	0.2
Dilation angle	30
Eccentricity	0.1 (default)
$F_{bo}/f_{co}$	1.16 (default)
Constant, $K_c$	0.6667 (default)
Viscosity	0 (default)

### 3.3.5 Meshing

#### a) Mesh size

Different analysis was done in validation work using different mesh size until the analysis result was conforming to experimental result obtained from the journal. So, 24mm mesh size gave the best result which conforms to the result obtained from the journal and takes reasonable running time for the model. Since dependent instances were used and mesh was done for parts.

#### b) Element type

For plain concrete column part C3D8R was used which are 8 nodes linear brick, reduced integration hourglass control element, outer and inner steel tubes were simulated by using Four-node solid elements with reduced integration (S4R) and for loading steel plates R3D4 which is a discrete rigid element were used. Finally, job was created and the result was taken when the analysis was completed. Though load vs axial displacement data was collected for each specimens. This load – displacement data was collected for all columns is presented in chapter four. The maximum loads were taken for quantification of the thickness, length and hollowness ratio effects.

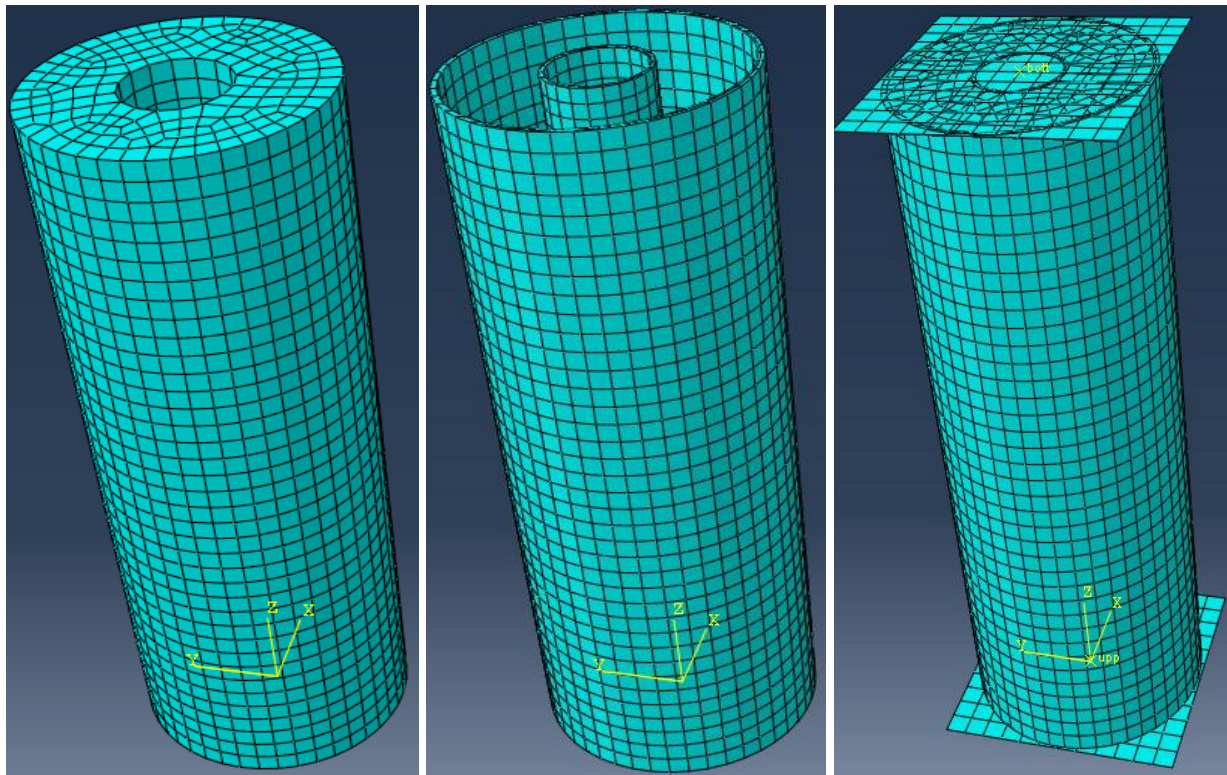


Figure 3.7: Finite element mesh for one of the CFDSSTC column analyzed.



### 3.3.6 Analysis step

In addition to initial steep only one step was created. In the created step static, riks method was selected. Static, Riks method includes material nonlinearity and also geometrical nonlinearity. By specifying maximum numbers of increments ABAQUS /Standard automatically chooses the size of the subsequent increments. Finally, the required field output and history was selected.

### 3.3.7 Boundary condition

A concrete filled double-skin steel tubular circular column was normally placed in to a testing machine and the load was applied on the specimens directly. To minimize the influence of end conditions on CFDSSTC columns, most researchers used end plates or stiffeners welded to both ends of a tube. For columns with welded end plates or stiffeners, there is no need to include the end plates or stiffeners in the model. Instead, the top and bottom surfaces of the steel tube and concrete can be fixed against all degree of freedom except for the displacement at the loaded end. In these research end plates was used to minimize the influence of end conditions on the specimens and to apply the load directly in to the columns.

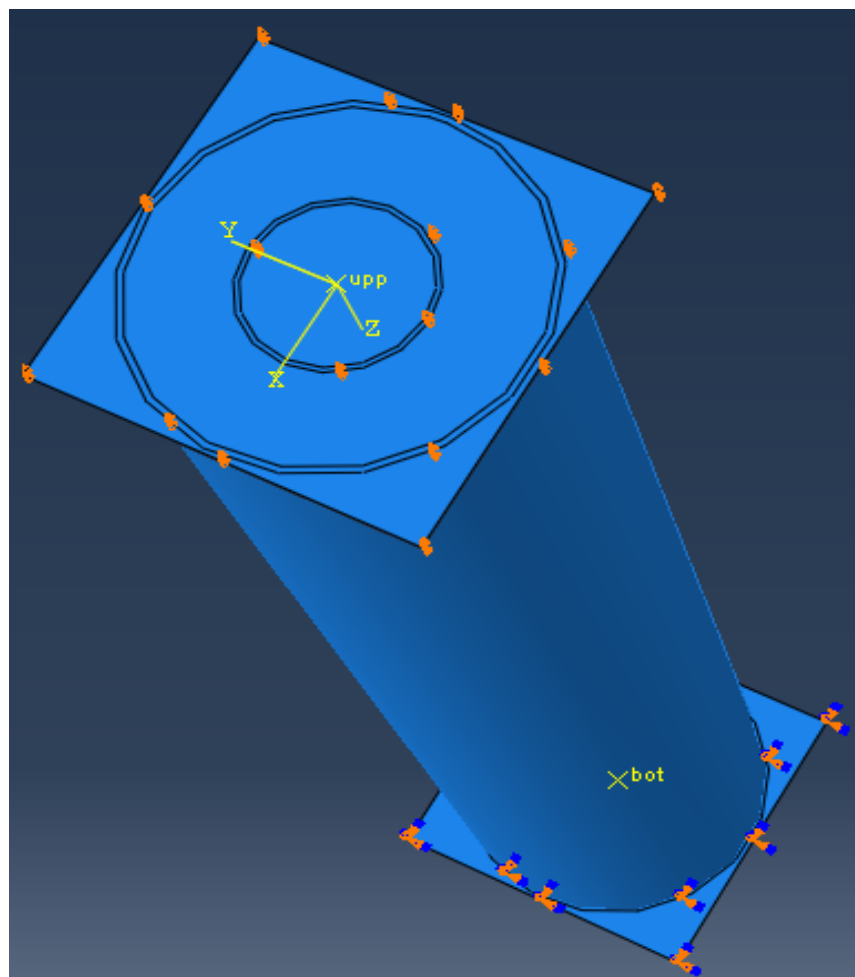


Figure 3.8: Boundary condition for one of CFDSSTC column analyzed.

### 3.3.8 Loading

The testing program was performed through universal loading system which applies the vertical load and the load was applied incrementally by subjecting a constant displacement through each cycle of loading. All the entire section of concrete filled double-skin steel tubular circular columns was loaded axially. In short axially loaded filled steel tube, the core concrete is acted upon by a confining stress, which results in higher axial strength of the column than another column. Displacement control method was adopted for loading. Loading was done for each specimen at the center. Load in (KN) and displacement in (mm) were automatically recorded by the system.

### 3.4 study variables

The study variables both dependent and independent were assessed in this research.

#### 3.4.1 Dependent variable:

The dependent variable of this study was:

- ✓ Axial load capacity of the column

#### 3.4.2 Independent variable:

The independent variables include:

- ✓ the hollowness ratio
- ✓ length of the column
- ✓ The outer and inner steel tube thickness.

### 3.5 Sample size and sampling procedures

The procedure utilized throughout the conduct of this research study was as follow: a continuous reviewed related literature on relevant areas of CFDSSTC columns under axial compression loads including articles, reference books, research papers, and standards specifications.

Based on the axial compression behavior of CFDSSTC columns, for the section which exhibits a failed and serious condition, an experimental (laboratory) investigation result was taken from the research and conducted analytical behavior of the columns. A conclusion and recommendation are drawn based on the results.

### 3.6 Data collection process.

Since this research was mainly about parameters affecting axial compression behavior of concrete filled double skin steel tubular circular columns. As a result, the only materials used in all of the models were concrete and steel.

The data for numerical analysis was obtained from ABAQUS and the secondary data was collected from literature.

#### 3.6.1 Materials properties

Steel strength: all structural steel members were taken  $f_yk = 375\text{Mpa}$  and  $f_yk=250\text{Mpa}$  for outer and inner steel tube respectively, which was obtained from the journal.

Concrete strength: concrete strength is classified according to the minimum 28 days crushing compressive strength of 150mm cubes in  $\text{N/mm}^2$ . All structural concrete members were used C25 for the all structural models.

### 3.7 Data processing and analysis.

The numerical analysis was done using ABAQUS and conducted by the procedure of software standards.

### 3.8 Data quality assurance

In order to assure data quality the following measure are taken:

- ✓ The ABAQUS software was checked for the known simple structural element to check whether it was working well or not.
- ✓ The loading and all structural modeling was double checked to remove errors.
- ✓ In case of any unreliable (illogical) results due to some unobserved errors, the structure was remodeled and reanalyzed.
- ✓ A due attention and care was taken when extracting results from ABAQUS and plotting them in Excel.

### 3.9 Validation of the model

Before starting modeling of all specimens, the validation work was done in order to decide on different parameters. The model with mesh size of 24mm had given the load that was closest to the experimental result (1188KN) obtained from the journal. The ultimate axial load resisting capacity of the model column found to be 1256.124KN. So, to evaluate the validation of the numerical model of the axially loaded CFDSSTC columns, the results from the numerical simulations of the experimental testing were compared with those from the experimental testing data obtained from the journal. The comparisons were carried out and the experimental result was about 87.57% of the FE results. The axial loads vs axial displacement curves of the FE analysis was matched with Axial load vs Displacement curves of the experimental result.

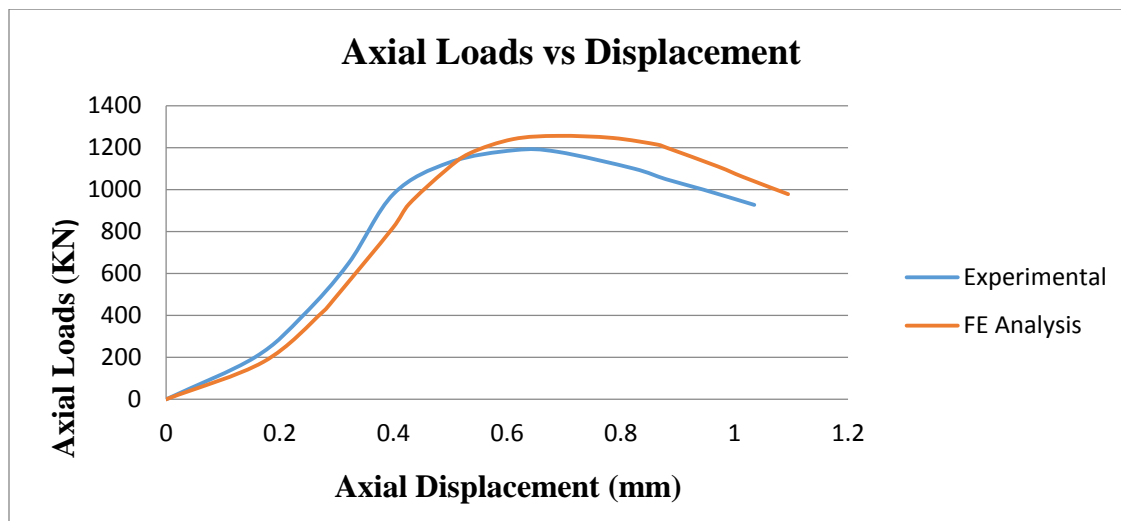


Figure 3.8: FE Load-Displacement curve vs experimental Load-Displacement curve.

## CHAPTER FOUR

### RESULT AND DISCUSSION

#### 4.1 Effects of hollowness ratio on the behavior of CFDSSTC columns.

According to axial load and axial displacement data taken from the software, hollowness ratio is an important parameter that affects CFDSSTC columns behavior. If hollowness ratio is equal to zero for a CFDSSTC column, the column is actually a conventional concrete-filled steel tube (CFST). This parameter was included in the analysis program to study its effect on the ultimate axial strength. Five CFDSSTC specimens named as (CFST-2, CFST-3, CFST-4, CFST-5, and CFST-6) with the same length, outer diameter and thickness, but with different hollowness ratio, the value of ( $\chi$ ) are (0, 0.25, 0.5, 0.75 and 1), respectively.

Load and displacement data for the specimens (CFST-2, CFST-3, CFST-4, CFST-5, and CFST-6) are presented in table 4.1.

Table 4.1: Load and Displacement data for (CFST-2, CFST-3, CFST-4, CFST-5, and CFST-6).

HR=0		HR=0.25		HR=0.5		HR=0.75		HR=1	
Disp.	Load	Disp.	Load	Disp.	Load	Disp.	Load	Disp.	Load
0	0	0	0	0	0	0	0	0	0
0.0621	142.514	0.0691	139.458	0.0721	127.459	0.0921	156.231	0.0782	94.125
0.1351	321.561	0.1154	246.125	0.1151	224.125	0.1351	246.125	0.1324	159.847
0.2135	526.325	0.2061	465.239	0.203	423.125	0.213	408.956	0.1858	230.154
0.3015	762.354	0.2723	610.458	0.2815	586.127	0.2714	510.124	0.3541	301.958
0.3795	943.621	0.3456	786.231	0.3538	746.329	0.3731	706.149	0.4847	432.368
0.3915	981.234	0.3945	896.235	0.4019	845.673	0.4124	793.486	0.4983	478.315
0.4698	1165.235	0.4665	1045.236	0.4679	985.126	0.4479	864.138	0.6371	513.146
0.5005	1231.514	0.5143	1140.569	0.5055	1037.458	0.5061	972.135	0.8356	622.315
0.5896	1436.251	0.6031	1310.841	0.5807	1178.457	0.6013	1146.325	0.9142	660.785
0.6795	1618.235	0.6954	1453.267	0.6365	1286.457	0.6272	1189.624	0.9854	716.125
0.7121	1684.235	0.7159	1489.561	0.6828	1362.514	0.7036	1317.125	1.1013	753.124
0.7941	1865.124	0.8124	1645.238	0.6952	1387.126	0.7258	1356.128	1.1288	799.439
0.8304	1936.215	0.8451	1684.125	0.8008	1568.541	0.7656	1411.854	1.1984	745.128
0.8534	1976.235	0.8701	1719.658	0.9147	1711.326	0.7952	1459.125	1.2169	723.629
0.8795	2004.635	0.88243	1729.568	0.9661	1742.918	0.8061	1472.365	1.2355	694.125
0.8959	2211.362	0.9654	1802.005	0.995	1716.32	0.861	1521.659	1.2754	645.128
1.0161	2304.193	1.0621	1862.655	1.0981	1623.154	0.981	1587.997	1.3167	587.169
1.1249	1765.239	1.1477	1635.124	1.2251	1326.154	1.1951	1145.236	1.3971	463.157
1.1925	1536.548	1.2482	1365.147	1.2592	1245.695	1.273	986.125	1.4451	386.245

Load and displacement data were taken from ABAQUS and the load vs displacement curves are drawn. From this curve, the ultimate loads were taken for all of the specimens and presented in tabular form as shown in table 4.2 and the load – displacement curves for the specimens is plotted and presented in figure 4.1.

Table 4.2: Axial load capacity of the specimens (for CFST-4 to CFST-8).

Specimens	Hollowness ratio	Ultimate load capacity (KN)
CFST-4	0	2304.193
CFST-5	0.25	1862.655
CFST-6	0.5	1742.918
CFST-7	0.75	1587.997
CFST-8	1	799.439

As shown in table 4.2 the axial strength decrease with the increase of hollowness ratio, this degradation in strength is almost linear when hollowness ratio change from 0% to 0.75%, where about 4.5% up to 11.5% loss in strength and the degradation in strength for hollowness ratio change from 0.75% to 1% was about 38.3% is occurred. Also it can be observed that the ultimate load decrease as the hollowness ratio increase.

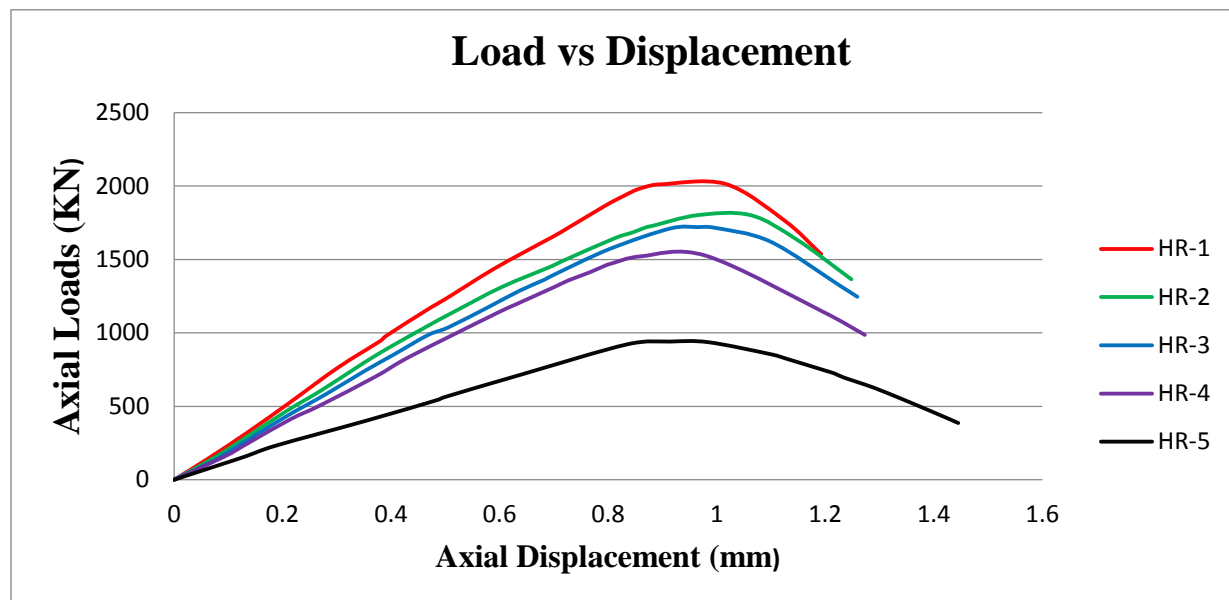


Figure 4.1: Load -Displacement curve for column (CFST-2 to CFST-6).

#### 4.2 Effects of outer steel tube thickness on the behavior of CFDSSTC columns.

The load – axial displacement curves of CFDSSTC specimens with outer steel tube thickness of 2mm up to 4mm are as shown in figure 4.3. It can be seen from the results that when the thickness of outer steel increase to 4mm, the ultimate load capacity of the specimens is increased by 7.55%, 4.84%, 6.18%, and 12.27% respectively. Therefore, the thickness of the outer steel tube has a great influence on the ultimate load capacity of the member.

Five CFDSSTC specimens name as (CFST-12, CFST-13, CFST-14, CFST-15, and CFST-16) with the same length, inner diameter and thickness, but with different thickness and diameter of outer steel, the value of outer tube thickness are (2mm, 2.5mm, 3mm, 3.5mm and 4mm), respectively. Load and displacement data for the specimens (CFST-12, CFST-13, CFST-14, CFST-15, and CFST-16) are as shown in table 4.3.

Table 4.3: Load Displacement data for columns (CFST-12 to CFST-16).

OST-1		OST-2		OST-3		OST-4		OST-5	
Disp.	Load	Disp.	Load	Disp.	Load	Disp.	Load	Disp.	Load
0	0	0	0	0	0	0	0	0	0
0.0857	122.365	0.0857	135.124	0.0857	145.695	0.0857	153.267	0.0857	183.264
0.1005	136.265	0.1003	154.126	0.1003	168.541	0.1006	182.695	0.1005	211.695
0.1321	186.594	0.1297	204.561	0.1365	224.598	0.1337	241.569	0.1351	272.154
0.2352	335.169	0.2342	359.124	0.2312	384.159	0.2311	425.624	0.231	463.125
0.3267	436.268	0.3017	457.169	0.3227	526.124	0.2536	459.847	0.3725	736.124
0.3492	461.597	0.3188	479.184	0.3765	607.158	0.3847	684.107	0.3841	756.317
0.4863	635.198	0.4853	683.125	0.4121	659.136	0.4577	813.074	0.4365	856.397
0.5041	653.126	0.4891	689.154	0.4741	754.139	0.4758	846.597	0.4841	962.873
0.5962	753.692	0.5836	807.456	0.5617	863.154	0.5902	1045.635	0.5273	1057.128
0.7096	896.235	0.6894	959.482	0.6596	1004.564	0.6004	1063.265	0.6306	1249.567
0.7413	936.126	0.7063	984.157	0.7441	1126.594	0.728	1245.635	0.748	1472.395
0.8365	1056.325	0.8276	1048.695	0.7654	1161.634	0.7312	1254.632	0.7565	1487.625
0.8922	1136.235	0.8684	1154.265	0.8252	1249.856	0.853	1436.235	0.8225	1597.263
0.9806	1236.564	0.9686	1211.06	0.8469	1286.514	0.8989	1521.036	0.8665	1674.891
1.0102	1274.365	0.9952	1285.412	0.9102	1376.514	0.9365	1578.564	0.9374	1784.562
1.1041	1365.236	1.0616	1365.128	1.0432	1565.344	0.9787	1601.365	0.9806	1810.561
1.1441	1387.457	1.1277	1404.265	1.1435	1465.312	1.0145	1621.272	1.0087	1838.773
1.1954	1341.235	1.1492	1487.530	1.2045	1345.187	1.1096	1615.324	1.1072	1823.954
1.2378	1236.148	1.1594	1301.265	1.2391	1265.415	1.1678	1532.104	1.2084	1563.259
1.2405	1236.845	1.2043	1278.965	1.2643	1204.156	1.2222	1387.072	1.2413	1451.267
1.3797	968.453	1.3109	1245.639	1.2914	1136.514	1.2674	1278.253	1.2597	1385.451



The ultimate loads were taken for all of the specimens for outer steel tube thickness and presented in table 4.4 as shown below.

Table 4.4: Axial load capacity of the specimens (CFST-12 TO CFST-16).

Specimens	Thickness of outer steel tube (mm)	Ultimate load capacity (KN)
CFST-14	2	1387.457
CFST-15	2.5	1487.530
CFST-16	3	1565.344
CFST-17	3.5	1621.272
CFST-18	4	1838.773

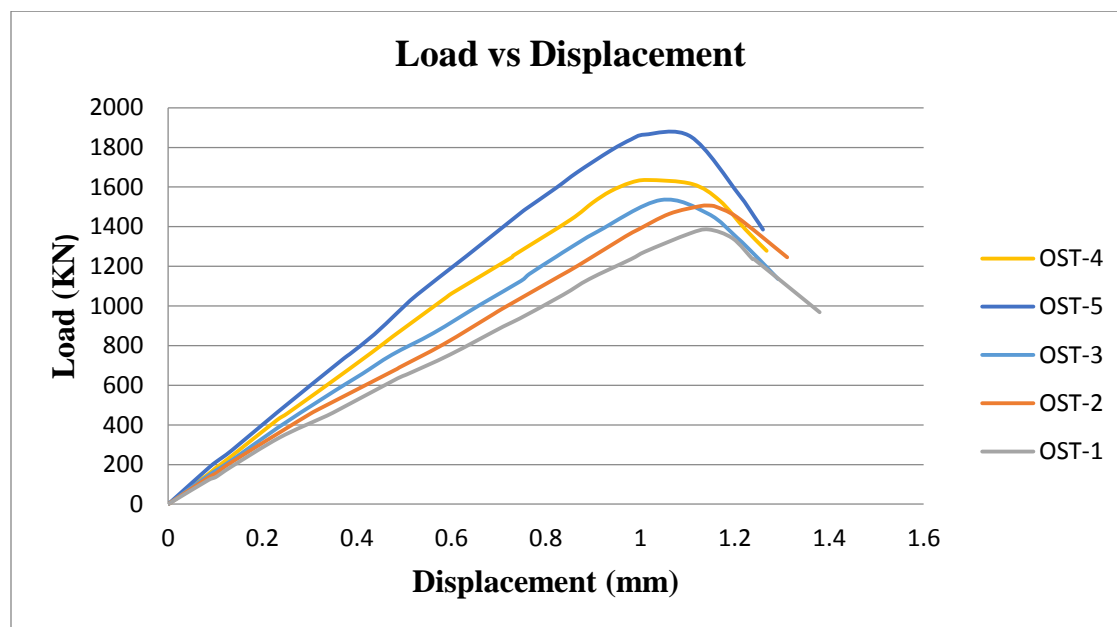


Figure 4.2: Load-Displacement curve for increasing outer steel tube thickness.

### 4.3 Effects of inner steel tube thickness on the behavior of CFDSSTC columns

As the thickness of inner steel tube of specimens (CFST-7, CFST-8, CFST-9, CFST-10, and CFST-11) increase from 2mm to 4mm, the ultimate load capacity also increased. Increasing the thickness of inner steel tube means an increase in the cross sectional areas, and then the axial strength of this tube increases in both case of acting alone or in composite action. Load and displacement data for the specimens (CFST-7, CFST-8, CFST-9, CFST-10, and CFST-11) are presented in table 4.5.

Table 4.5: Load and displacement data for specimens (increasing inner steel tube thickness).

IST-1		IST-2		IST-3		IST-4		IST-5	
Disp.	Loads	Disp.	Loads	Disp.	Loads	Disp.	Loads	Disp.	Loads
0	0	0	0	0	0	0	0	0	0
0.1391	186.325	0.1329	190.351	0.11702	184.235	0.116	198.125	0.0991	199.539
0.1896	249.367	0.1796	253.885	0.1534	245.632	0.1554	265.135	0.1596	297.206
0.3035	399.078	0.2738	378.459	0.2616	389.265	0.2341	379.168	0.2235	399.078
0.3315	439.268	0.3319	469.235	0.3002	450.863	0.2826	456.326	0.2515	445.129
0.4112	562.349	0.4018	586.948	0.3593	551.055	0.3486	576.238	0.2912	523.624
0.4525	627.391	0.4322	641.655	0.4318	680.209	0.4112	689.123	0.3725	674.126
0.5293	759.634	0.5062	776.235	0.5083	816.25	0.4467	756.326	0.4193	784.125
0.5926	874.236	0.5526	855.543	0.5591	924.107	0.4842	836.129	0.4326	818.779
0.6531	990.687	0.6337	1023.625	0.5999	1008.117	0.5421	974.136	0.4931	982.535
0.6957	1089.756	0.6785	1129.365	0.6531	1157.532	0.6001	1123.698	0.5557	1146.291
0.7403	1197.234	0.7207	1238.125	0.7006	1268.369	0.6642	1299.843	0.6203	1310.047
0.7865	1296.247	0.7367	1283.311	0.7714	1446.915	0.7231	1463.294	0.6865	1473.803
0.8412	1425.872	0.8126	1456.948	0.8434	1623.514	0.7541	1563.126	0.7421	1637.559
0.9148	1516.312	0.8737	1589.398	0.8812	1698.265	0.7913	1653.259	0.8032	1801.315
0.9647	1555.496	0.9459	1711.081	0.90535	1736.268	0.8154	1703.262	0.8256	1868.659
1.0111	1535.987	1.0305	1769.177	0.9943	1834.023	0.8821	1822.65	0.9003	2013.635
1.0131	1528.549	1.1314	1536.248	1.0723	1635.124	1.0012	1857.564	1.0101	2058.655
1.0765	1513.658	1.1602	1468.367	1.1114	1536.231	1.1521	1546.935	1.1265	1745.235
1.1293	1436.268	1.1781	1418.368	1.1453	1456.235	1.1747	1485.625	1.1893	1563.268

The ultimate loads were taken for all of the specimens for inner steel tube thickness are presented in tabular form as shown in table below

Table 4.6: Axial load capacity of the specimens for inner steel tube thickness.

Specimens	Thickness of inner steel tube ( $t_i$ )	Ultimate load capacity (KN)
CFST-9	2	1555.496
CFST-10	2.5	1769.177
CFST-11	3	1834.023
CFST-12	3.5	1857.564
CFST-13	4	2058.655

As seen in table 4.6 above, percentage increase in axial capacity of a column for increasing thickness from 2mm – 4mm, was 3.13%, 2.52%, 4.42%, and 8.73% respectively. The load – displacement curves for the specimens is plotted and presented in figure 4.3.

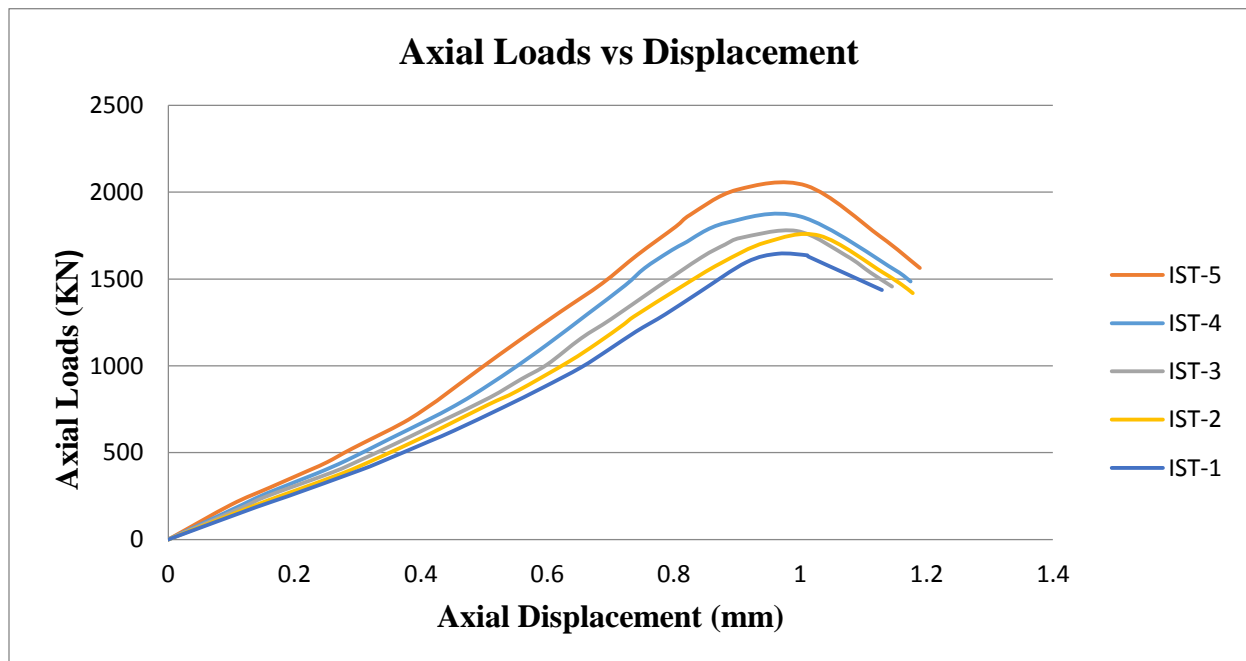


Figure 4.3: Load-Displacement curve for the specimens (increasing inner steel tube thickness).

#### 4.4 Effects of length of the columns on the behavior of CFDSSTC columns.

As shown in figure 4.5, the load vs displacement graph for different length of the CFDSSTC column with the same outer tube diameter and thickness, and inner tube diameter and thickness. The percentage decrease in axial strength of columns for increasing length from 1m to 4m was 3.54%, 5.82%, 6.07%, 8.02%, 7.04%, 5.32% respectively. This indicates that the column expected to decrease in axial strength when the length of the column increases from 1000mm to 4000mm. The ultimate loads were taken for all of the specimens for increasing length of the columns and presented in tabular form as shown in table 4.7 below.

Table 4.7: Ultimate load capacity of the specimens with increasing length of the column.

Specimens	Length of the column (mm)	Ultimate load capacity (KN)
CFST-17	1000	2965.182
CFST-18	1500	2758.349
CFST-19	2000	2537.656
CFST-20	2500	2434.391
CFST-21	3000	2323.185
CFST-22	3500	2109.220
CFST-23	4000	2025.359

The load – displacement curves for the specimens is plotted and presented as shown in figure 4.4.

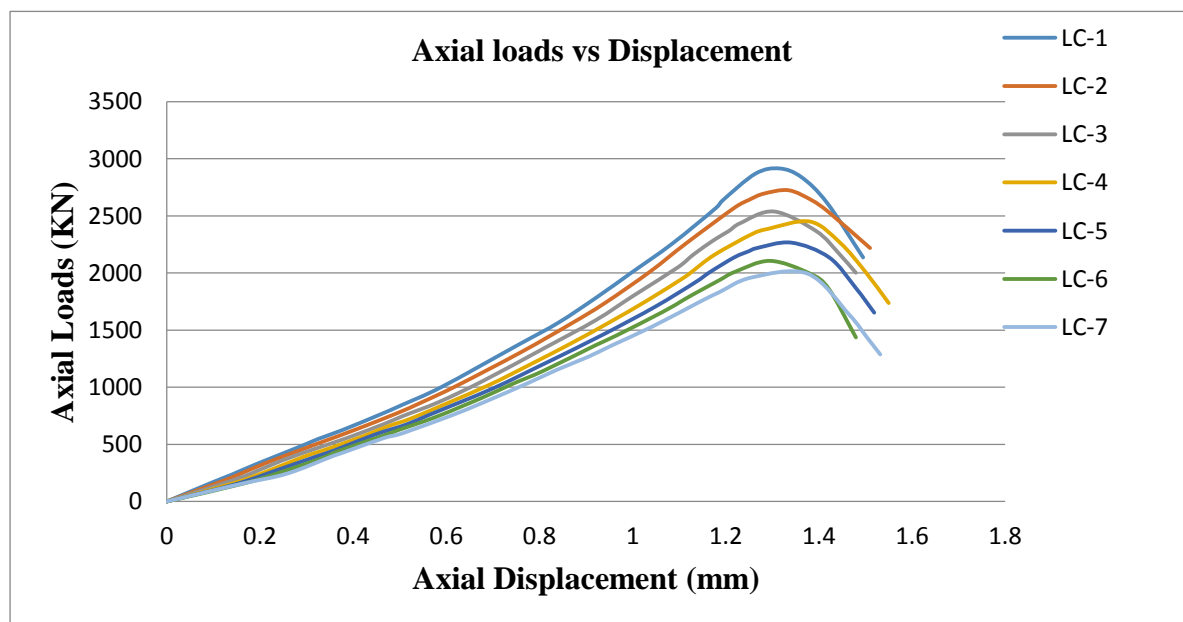


Figure 4.4: Load-Displacement curve for column with increasing length.

Load and displacement data for the specimens (CFST-17, CFST-18, CFST-19, CFST-20, and CFST-21) are tabulated in table 4.8.

Table 4.8: Load-Displacement data for the specimens (increasing length of the column).

LC-1		LC-2		LC-3		LC-4		LC-5		LC-6		LC-7	
Disp	load	Disp	load	Disp	load	Disp	load	Disp	load	Disp	load	Disp	load
0	0	0	0	0	0	0	0	0	0	0	0	0	0
0.0967	165.298	0.1167	174.265	0.1407	183.647	0.1408	156.327	0.1456	148.629	0.1625	154.635	0.1581	152.314
0.1405	236.659	0.1505	228.947	0.1804	243.519	0.2105	256.329	0.2454	286.549	0.2554	269.548	0.2585	243.625
0.1921	326.985	0.2121	335.129	0.2462	356.128	0.2931	389.257	0.3225	395.623	0.3361	384.265	0.3554	395.627
0.2852	478.695	0.2932	459.637	0.3236	468.237	0.3465	461.238	0.3614	449.632	0.3668	438.627	0.3758	423.657
0.3267	549.638	0.3437	536.149	0.3863	554.391	0.4225	572.168	0.4461	584.163	0.4654	576.213	0.4659	554.692
0.3763	623.598	0.4057	629.416	0.4667	678.239	0.4751	658.125	0.5151	674.235	0.4965	623.549	0.4963	584.128
0.4572	759.394	0.4926	769.359	0.5061	746.329	0.5306	736.259	0.5625	756.298	0.5789	741.27	0.5256	625.351
0.5056	845.693	0.5463	865.603	0.5839	869.613	0.6862	1008.698	0.6984	985.635	0.6798	912.475	0.6058	744.029
0.5913	1004.562	0.6232	1014	0.6801	1057.102	0.7811	1200.354	0.8058	1196.32	0.7387	1022.25	0.6789	865.041
0.7522	1365.485	0.7601	1305.46	0.8122	1345.683	0.8702	1388.118	0.8258	1235.7	0.8095	1144.77	0.7759	1036.548
0.8406	1564.158	0.8661	1551.18	0.9209	1586.118	0.9501	1566.678	0.9381	1463.03	0.9196	1365.21	0.8387	1154.256
0.9241	1789.653	0.9401	1735.01	1.0013	1799.003	1.0304	1755.658	1.0487	1704.33	0.9656	1452.64	0.9048	1265.837
0.9974	2001.456	1.0371	2009.41	1.0976	2049.365	1.1101	1958.564	1.1361	1921.22	1.0648	1658.39	0.9558	1365.894
1.0854	2256.418	1.1154	2260.02	1.1305	2160.018	1.1254	2003.658	1.1658	2006.31	1.1065	1756.33	1.0435	1532.247
1.1795	2569.845	1.2204	2574.84	1.1757	2290.145	1.1751	2156.415	1.2187	2136.55	1.1279	1806.75	1.1454	1749.259
1.1937	2635.458	1.2507	2640.45	1.2063	2365.478	1.2563	2339.548	1.2495	2189.63	1.1865	1936.67	1.1854	1829.564
1.2641	2869.124	1.2821	2694.13	1.2314	2435.654	1.2909	2385.624	1.2654	2215.68	1.2203	2009.9	1.2556	1959.991
1.3156	2965.182	1.3352	2758.35	1.3039	2537.656	1.3812	2434.391	1.3406	2323.19	1.2954	2109.22	1.3761	2025.359
1.3625	2839.137	1.3854	2635.15	1.3949	2365.014	1.4461	2263.004	1.4225	2135.07	1.3801	1996	1.4653	1635.214
1.4175	2614.983	1.4201	2536.25	1.4443	2165.326	1.5013	2003.451	1.4801	1865.26	1.4212	1862.54	1.5035	1435.629
1.4952	2135.629	1.5101	2218.13	1.4795	2001.659	1.5501	1736.265	1.5191	1652.36	1.4797	1435.63	1.5321	1286.354

#### 4.5 Modes of failure

As shown in figure 4.5, 4.6, and 4.7 most of the failure of the CFDSSTC specimens is mainly due to crushing of concrete at mid height and the yielding of the outer steel tube, which is mainly due to the combined effect of axial compression loads and expansion of the in-filled concrete. No failure was found in the inner steel tube.

The CFDSSTC columns of HR=1 was failed by steel tube buckled outward and 1.5m, 2m, 2.5m, 3m, 3.5m, and 4m length specimens failed by crushing of concrete at mid height and a little buckling outward of the outer steel tube. All the yielding of the steel tubes occurs in short column are in the upper part.

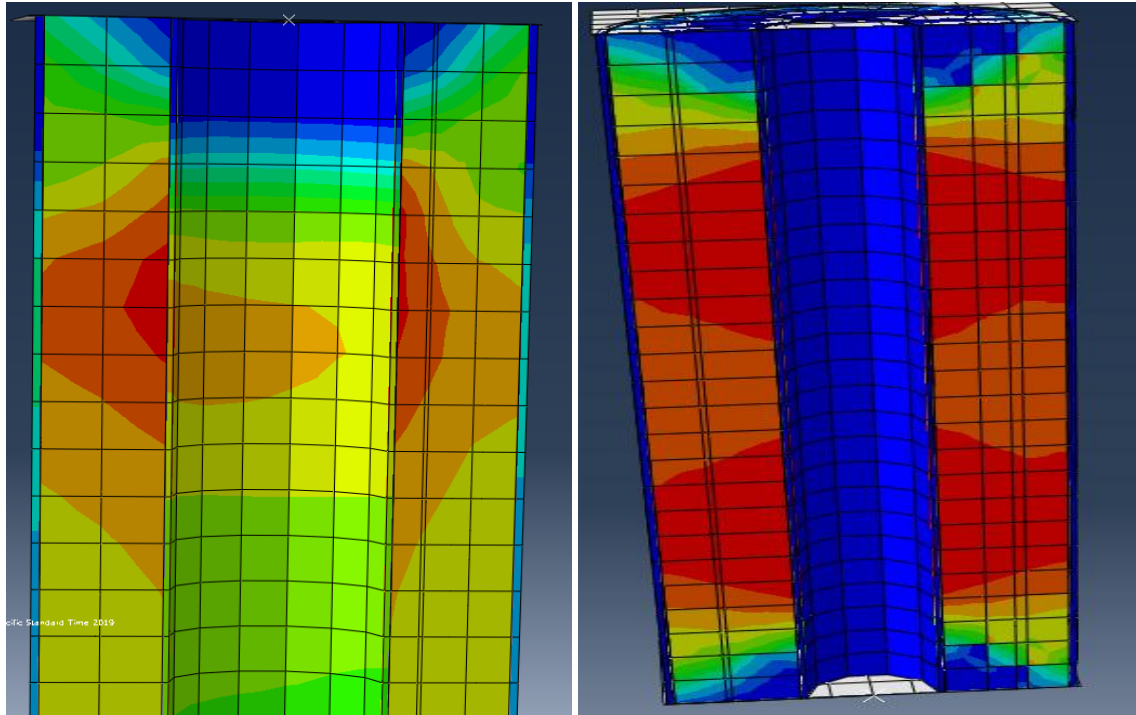


Figure 4.5: Failure on OST=3mm specimens. Figure 4.6: Failure on 0.6mm specimens.

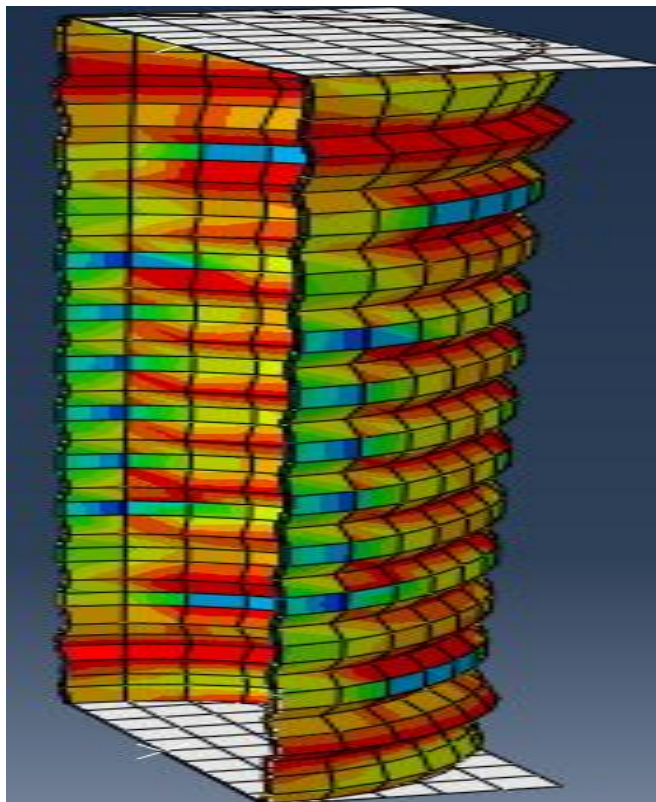


Figure 4.7: Failure on HR=1 CFDSSTC columns.

## CHAPTER FIVE

### CONCLUSION AND RECOMMENDATION

#### 5.1 Conclusion

This paper has presented non-linear finite element analysis of concrete filled double skinned steel tubular circular column under axial compression loads. The analysis involved twenty three different specimens were modeled and analyzed on ABAQUS, to investigate the behavior, the ultimate load carrying capacity and the effect of the key parameter on the axial load-displacement relationship of the column. Before modeling of the whole specimens one CFDSSTC columns was modeled and analyzed for validation. The validation results show that the experimental ultimate strength of the column was 87.57% of FE strength of the same column. The key parameters studied were hollowness ratio varies from 0 - 1 with a constant interval of 0.25, outer and inner steel tube thickness range from 2mm - 4mm with a constant interval of 0.5mm, and length of the columns range from 1m – 4m with an interval of 0.5m. On the base of the results presented in this paper, the following conclusions can be drawn.

- ✓ Columns under increasing hollowness ratio demonstrates an almost decreasing the ultimate load carrying capacity of the specimens, this degradation in strength is almost linear when hollowness ratio change from 0 to 0.75, where about 4.5% up to 11.5% loss in strength and the degradation in strength for hollowness ratio change from 0.75 to 1 was about 38.3% is occurred.
- ✓ Inner and outer steel tube thickness has a significant influence on the axial loads-displacement behavior of CFDSSTC columns. As expected, increasing the outer and inner steel tube thickness leads to increase in the axial load carrying capacity of the specimens. It can be seen from the results that when the thickness of outer steel tube increase to 4mm, the ultimate load capacity of the specimens was increased by 7.55%, 4.84%, 6.18%, and 12.27% and percentage increase in axial capacity of a column for increasing thickness of inner steel tube from 2mm – 4mm, was 3.13%, 2.52%, 4.42%, and 8.73% respectively.



- ✓ Increasing the length of CFDSSTC columns leads to a decrease in the ultimate axial load carrying capacity. The percentage decrease in axial strength of columns for increasing length from 1m to 4m was 3.54%, 5.82%, 6.07%, 8.02%, 7.04%, 5.32% respectively. This indicates that the column expected to decrease in axial strength when the length of the column increases from 1000mm to 4000mm.
- ✓ Most of the failure of the CFDSSTC specimens is mainly due to crushing of concrete at mid height and the yielding of the outer steel tube, which is mainly due to the combined effect of axial compression loads and expansion of the in-filled concrete. No failure was found in the inner steel tube.

## 5.2 Recommendation

The following recommendations are suggested for further studies:

- ✓ In this study only circular CFDSST columns were investigated. Therefore it's recommended if columns with different shape are investigated for axial compression behavior of CFDSST columns.
- ✓ Experimental and numerical studies on changing grade of concrete should be performed on this parametric study.
- ✓ Effect of confinement co-efficient and its value is another important focus of this area.
- ✓ The study considered only the effect of concentric axial load on ultimate load capacity of the column. However, in real life situations, many columns are subject to eccentric loading due to different situation. Therefore, the study can be furthered by incorporating the influence of eccentric axial load on ultimate load resisting capacity of the columns.

**REFERENCE**

- [1] S.Mathankumar and M. Anbarasan. Finite Element Analysis of steel tubular section filled with concrete.2016; Vol 5: issued 6.
- [2] C.X.Dong and J.C.M. Ho. Concrete-filled double-skin tubular Columns with external steel rings. Australian Earthquake Engineering Society 2012 Conference.
- [3] ELchalakani,M, Zhao XL and Grzebieta RH. Test on concrete filled double-skin (CHS outer and SHS inner) composite under axial compression. 2002; Vol 5; pp: 415-419.
- [4] Shanthosh Kumar, D and Gmohan Ganesh. Experimental investigation of composite steel-concrete column. 2014; Vol 2: issue 5.
- [5] P.Nivetha and V.Anandhi. Experimental investigation on steel concrete composite stubs. IJESC. 2017; vol 07; issue 04.
- [6] Abbas S.A. AL-Ameeri and Safa M.N. Ahmed. Improving the resistance of self-compacting concrete exposed to elevated temperatures by using steel fiber. ISSN 2224-5790. 2013; Vol3; No 13.
- [7] Beena Kumari. Concrete filled steel tubular (CFST) columns in composite structures. IOSR Journal of Electrical and Electronic Engineering (IOSR-JEEE); 2018. E-ISSN: 2278-1676, P-ISSN: 2320-3331, Vol 13, issue 1.
- [8] Shakir- Khalid, H. and Zeghiche, J. Experimental behavior of concrete-filled rolled rectangular hollow-section columns. The structural Engineer, 67(19), pp: 346-353.
- [9] Gourley, B. C., Tort, C., Hajjar, J. F. and Schiller, P. H. A synopsis of studies of the monotonic and cyclic behavior of concrete-filled steel tube beam-columns. Structural Engineering Report No. ST-01-4. Institute of Technology, University of Minnesota. 2001.
- [10] Huang, C. S., YEH, Y.K.,Liu, G. Y., Hu, H. T., Tsai, K. C., Weng, y. t., Wang, s. h. and Wu, M. H. Axial load behavior of stiffened concrete-filled steel columns. Journal of structural Engineering; 2002. Pp: 1222-1230.
- [11] Mursai Mohanad. The behavior and design of thin walled concrete filled steel box columns. Ph. D. thesis; 2007; Sydney, Australia.
- [12] Tomii, M. ductility and strong columns composed of steel tube, infilled concrete and longitudinal steel bars. Proceedings of the third International conference on steel-concrete composite structures. 1991; Fukuoka, Japan; pp: 39-67.

- [13] Han, T.H, Stallings, J.M and Kang, Y.J. Nonlinear concrete model for double-skinned composite tubular columns. *Journal of construction and building materials*. 2010; Vol 24; No 12; pp: 2542-2553.
- [14] Dr. R iyadah, J., Dr. Laith, K. Al-Hadithy Shayma. M. Behavior of concrete filled double skin steel tubular column under static axial compression load. *Journal of Engineering and development* . 2016; Vol 20; No 02; ISSN: 1813-7822.
- [15] Ermiyas Ketema. Design aid for composite columns. Msc thesis. 2005.
- [16] C.X. Dong and J.C.M. Ho. Concrete-filled double-skin tubular columns with external steel rings. Australian earthquake Engineering society 2012 conference. Dec 7-9; Gold Coast, Qld.
- [17] Mohammed Mahmoud EL-Heweity. On the performance of circular concrete-filled high strength steel columns under axial loading. *Journal of Alexandria Engineering*. 2012; pp: 109-119.
- [18] Nardin, S. D. and EL Debs, A. L. H. C. Axial load behavior of concrete-filled steel tubular columns. *Proceeding of the institution of civil engineers, structures and Building*. 2007; pp: 13-22.
- [19] N. Umamaheswari, S. Arul Jayachandran. Influence of concrete confinement on axial load capacity of concrete –filled steel tubes. *Journal of civil Engineering research*. 2014; pp: 12-16.
- [20] Hu, H.T., Huang, C.S., Wu, M.H. and Wu, Y.M. Nonlinear analysis of axially loaded concrete filled tube columns with confinement effect. *Journal of structural Engineering*. 2003; pp: 1322-1329.
- [21] Shanmugam, N.E. and Lakshmi, B. State of the art report on steel concrete composite columns. *Journal of constructional steel research*. 2001; pp: 1041-1080.
- [22] Oehlers, D. J. and Bradford, M.A. Composite steel and concrete structural members:Fundamental behavior. Pergamon. 1995.
- [23] Uy, B. concrete-filled fabricated steel box columns for multi-storey buildings: behavior and design. *Progress in structural Engineering and Materials*. 1998; Vol 1;No; 2; pp:150-158.
- [24]. Bradford, M.A.and Oehlers, D. J. Composite steel and concrete structural members:Fundamental behavior. Pergamon. 1995.
- [25] Ivan M. Viest et al. Composite columns in composite construction design for buildings. ASCE, Mc GRAW-Hill, New York. 1997; pp: 4.1-4.51.

- [26] Mathias Johansson and Kent Gylltoft. Structural behaviour of slender circular steel-concrete composite columns under various means of load application, steel and composite structures. Chalmers University of technology, Sweden. 2001; Vol 1; No 4.
- [27] Dr. S. Prabhavathy and D. Surendar. Comparative study of concrete filled tubes with hollow double skinned composite columns in-filled with self-compacting concrete. Proceedings of international conference on advances in architectural and Civil Engineering (AARCV). 2012; paper ID SAM178; Vol 1.
- [28] JF Hajjar. Concrete filled steel tube columns under earthquake loads. Prog structural Engineering material. 2000; [www.hosted.ce.umn.edu](http://www.hosted.ce.umn.edu).
- [29] K. Rajasekar, N. SAKthieswaran, G. Shiny Brinthan and O. Ganesh Babu. Study about the behavior of concrete filled tubular column with GFRP wrapping. IJRASET. 2016; Vol 4; No 5; ISSN: 2321-9653.
- [30] Zhao, X-L., Grzebieta, R. and Elchalakani, M. (2002). Test of concrete-filled double skin CHS composite stub columns. Jsteel and composite structures, 2: 129-146.
- [31] Mohammed H. Shams. Non-linear evaluation of concrete-filled steel tubular columns. New Jersey institution of technology. January 1997, Iran.
- [32] Hasan Hastemoglu. Behaviour of double skinned composite columns with concrete filled tubular columns. Journal of Architectural Engineering technology. 2017; Vol 6; No 2.
- [33] Dr. Riyadh J. Aziz, Dr. Laith Kh. Al-Hadithy and Shayma M. Resen. Behaviour of concrete filled double skin steel tubular columns under static axial compression load. Journal of Engineering and development. 2016; Vol 20; No 02; ISSN: 1813-7822
- [34] Shigana Abdul Karim, Beenet Aipe. Comparative study on CFRP concrete filled double skin tube (CFDST) columns. 2016; Vol 3; No 4; ISSN: 2349-6002.
- [35] Dr.S. prabhavathy and D.Surendar. Comparative study of concrete filled tubes with hollow double skinned composite columns in-filled with self-compacting concrete. 2012; Vol 1; No 5; SAM 178.
- [36] Fujimoto, T., Mukkai, A., Nishiyama, L. and Sakino, K, behaviour of eccentrically loaded concrete-filled steel tubular columns. Journal of structural Engineering. 2004; pp: 203-212.
- [37] Shigana Abdul Karim, Bennet.A. Comparative study on CFRP concrete filled double skin tube (CFRST) columns. 2016; Vol 3; No 4; ISSN: 2349-6002.

[38] Han LH, Yao GH, Tao Z. performance of concrete filled thin-walled steel tubes under pure torsion. *Thin-walled struct.* 2007; pp: 24-36.

[39] Alfarah B, Lopez-Almense F, Oller. S. New method for calculating damage variables evaluation in plastic damage model for RC structures. *Journal of Engineering structures.* 2017. Pp: 70-86.

## APENDIX A

## MATERIAL PROPERTIES

## A.1 Concrete properties

Table A.1: Compressive stress-total strain of concrete.

$\sigma_c$	$\epsilon_c$
14.34701201	0
19.92898409	0.000116848
24.48583677	0.000222074
28.04336806	0.00035905
30.6265175	0.000526982
32.25940163	0.000725105
32.96534764	0.000952677
33	0.001020942
32.76692539	0.001208981
31.6859779	0.001493323
29.7436504	0.001805031
26.96041794	0.002143456
23.35611175	0.002507966
18.94994436	0.002897952

Table A.2: Compressive stress-crushing strain.

$\sigma_c$	$\epsilon_{in}$
14.34701201	0
19.92898409	0.116847541
24.48583677	0.222074357
28.04336806	0.359050047
30.6265175	0.52698227
32.25940163	0.725104834
32.96534764	0.952676623
33	1.020941951
32.76692539	1.208980584
31.6859779	1.493322754
29.7436504	1.80503134
26.96041794	2.143455842
23.35611175	2.507966211
18.94994436	2.897952058

Table A.3: Concrete damage variable vs crushing strain.

Dc	ein
0	0.044189213
0	0.116847541
0	0.222074357
0	0.359050047
0	0.52698227
0	0.725104834
0	0.952676623
0	1.020941951
0.007062867	1.208980584
0.039818851	1.493322754
0.098677261	1.80503134
0.183017638	2.143455842
0.292239038	2.507966211
0.425759262	2.897952058

Table A.4: Tensile stress-cracking strain of concrete.

$\sigma_t$	$\epsilon_t$
2.56496392	0
1.638124916	0.000197956
1.241466537	0.000460558
1.055597892	0.000716463
0.940855698	0.000970109
0.860516128	0.001222661
0.799993606	0.001474584
0.752155785	0.001726104
0.713035284	0.001977347
0.703376857	0.00204702
0.680220964	0.002228389
0.652149275	0.002479281
0.627754655	0.002730056
0.606281781	0.002980738
0.587177865	0.003231345
0.570027492	0.00348189



Table A.5: Tensile damage variables-cracking strain of concrete.

Dt	$\sigma_t$
0	2.56496392
0.361345825	1.638124916
0.515990643	1.241466537
0.588455072	1.055597892
0.6331895	0.940855698
0.66451141	0.860516128
0.688107267	0.799993606
0.706757752	0.752155785
0.722009624	0.713035284
0.725775146	0.703376857
0.734802911	0.680220964
0.745747193	0.652149275
0.7552579	0.627754655
0.763629509	0.606281781
0.771077534	0.587177865
0.777763934	0.570027492

## APENDEX B

Axial loads for all CFDSSTC columns

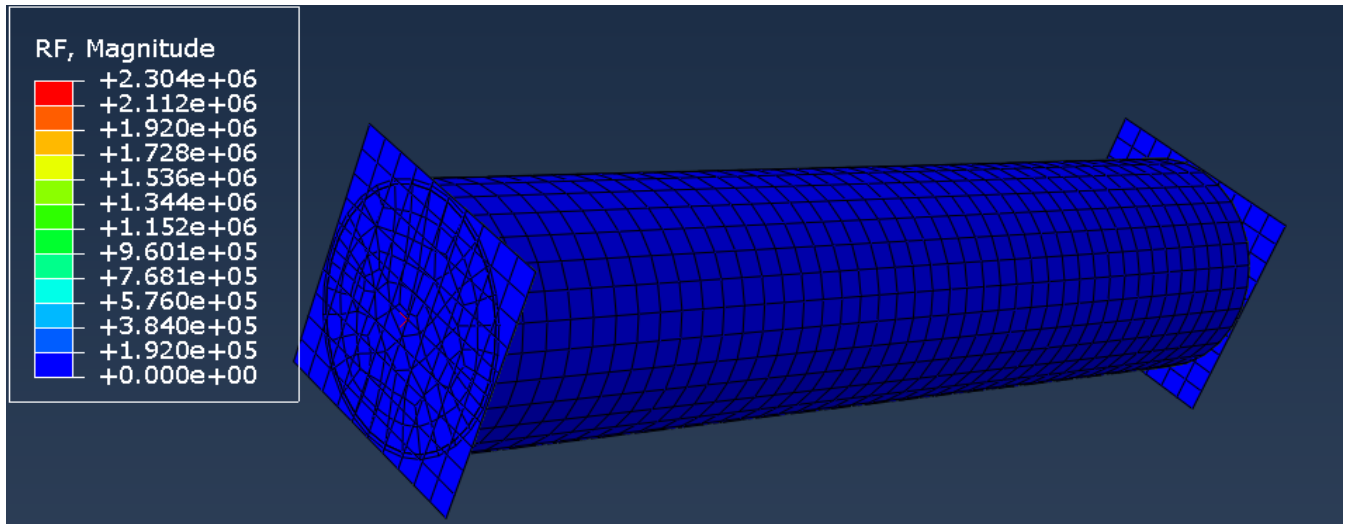


Figure B.1: Axial loads for HR=0 CFDSSTC columns.

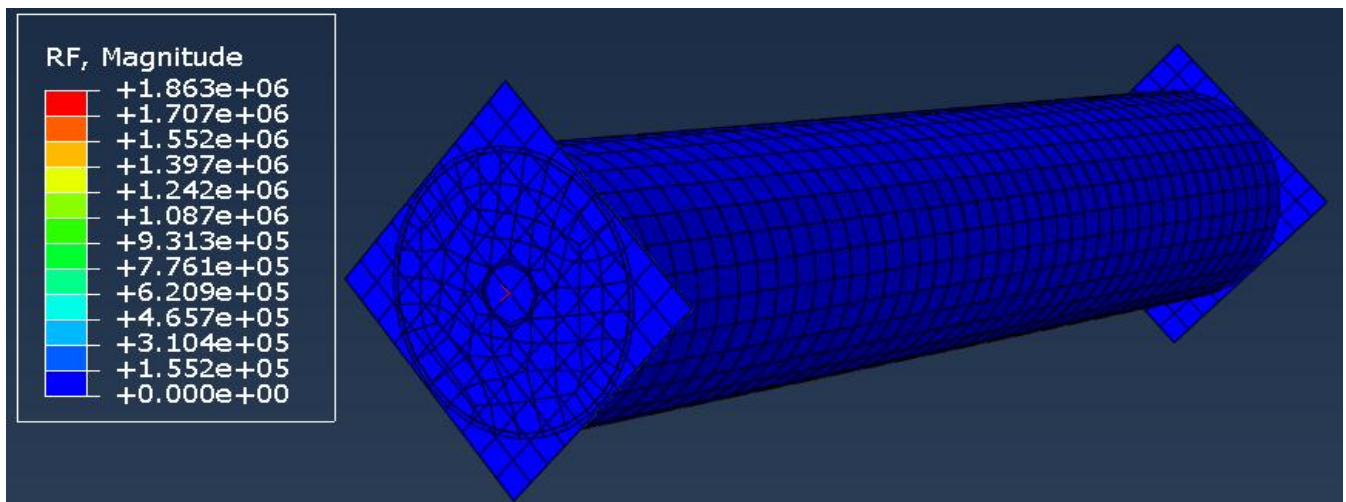


Figure B.2: Axial loads for HR=0.25 CFDSSTC columns.

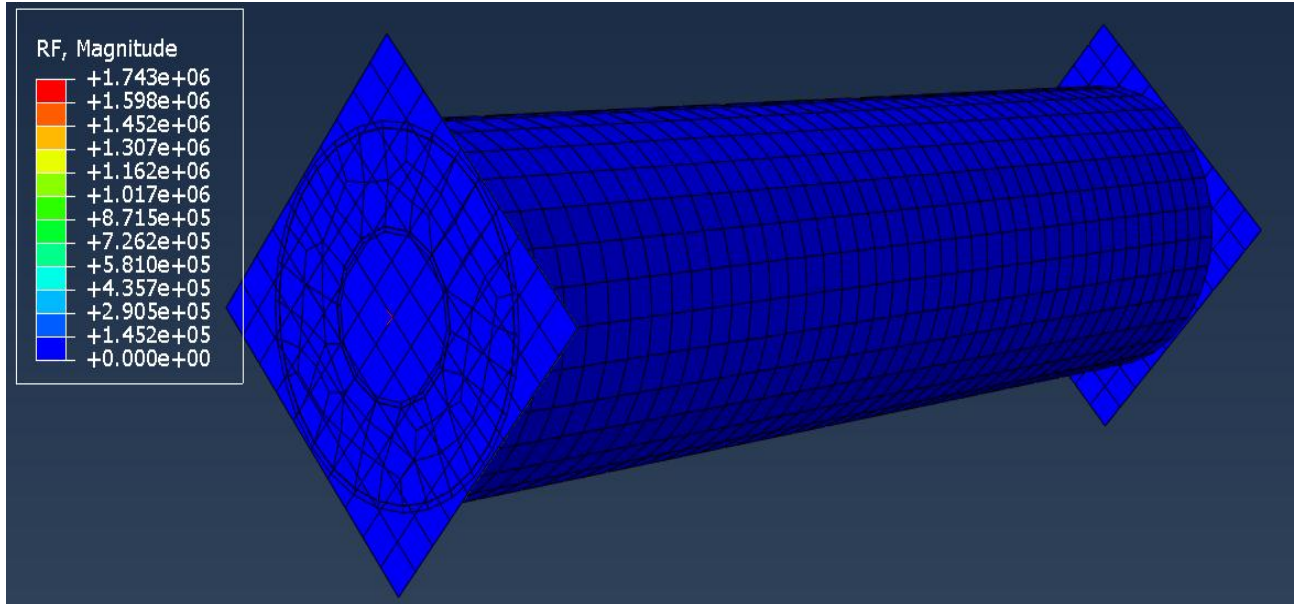


Figure B.3: Axial loads for HR=0.5 CFDSSTC columns.

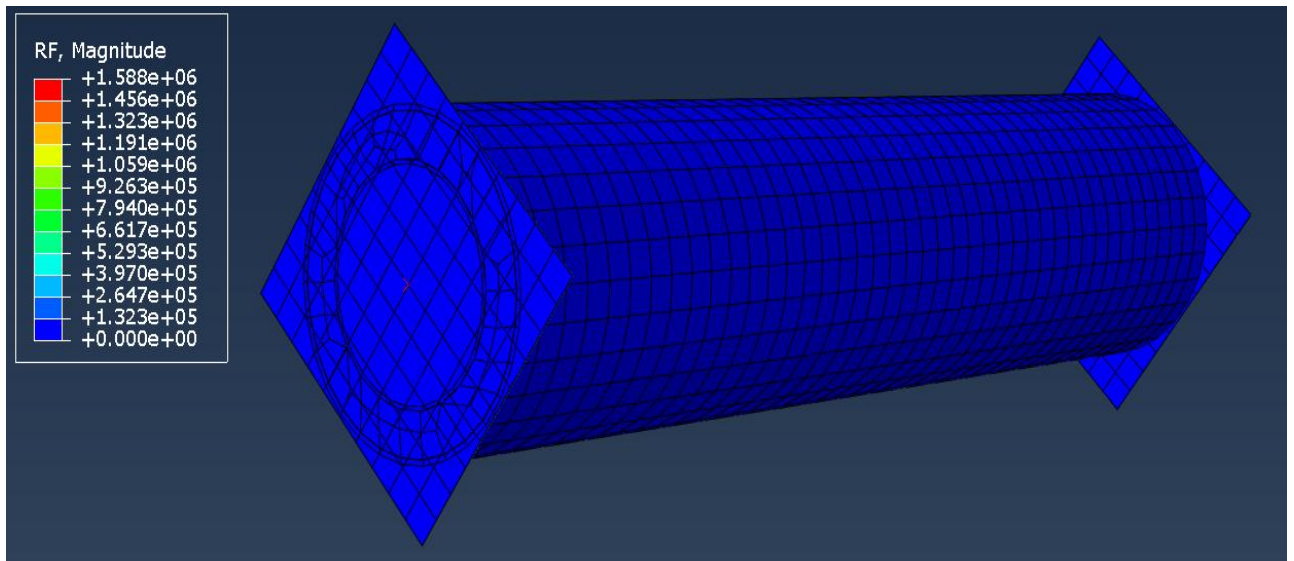


Figure B.4: Axial loads for HR=0.75 CFDSSTC columns.

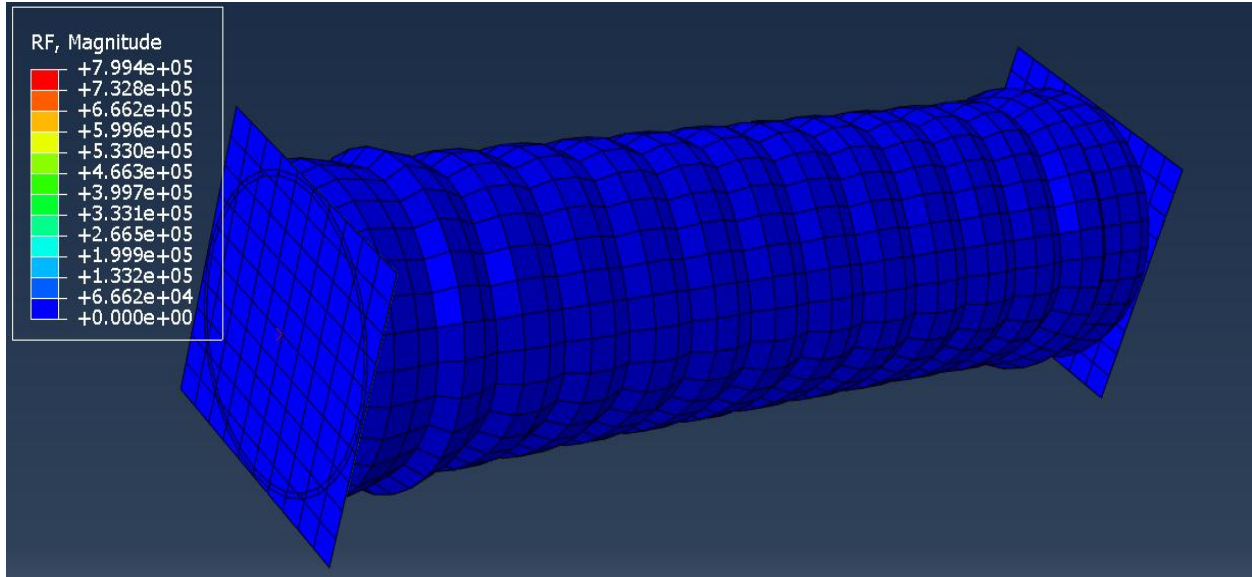


Figure B.5: Axial loads for HR=1 CFT columns.

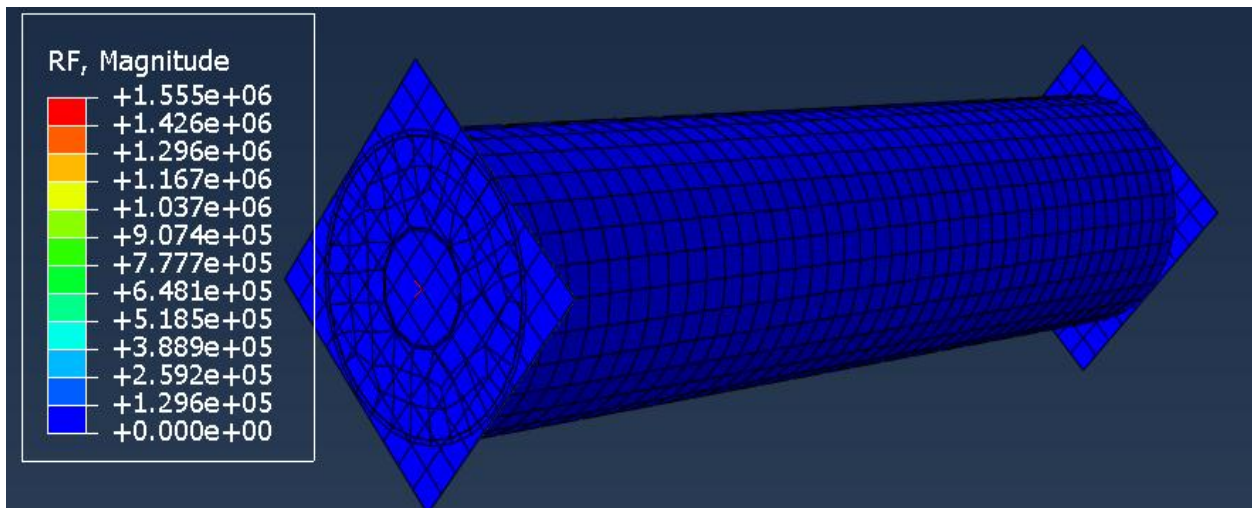


Figure B.6: Axial loads for IST=2mm CFDSSTC column.



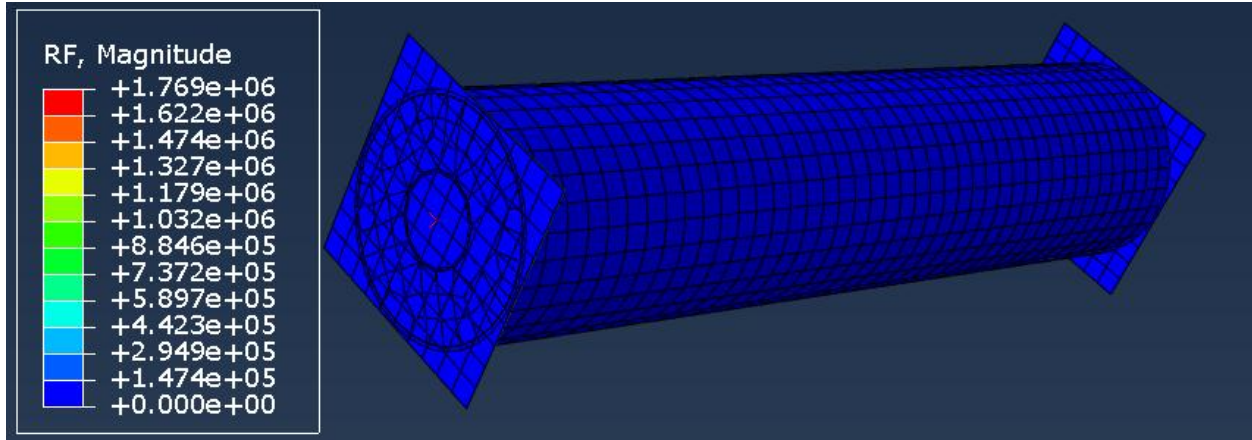


Figure B.7: Axial loads for IST=2.5mm CFDSSTC column.

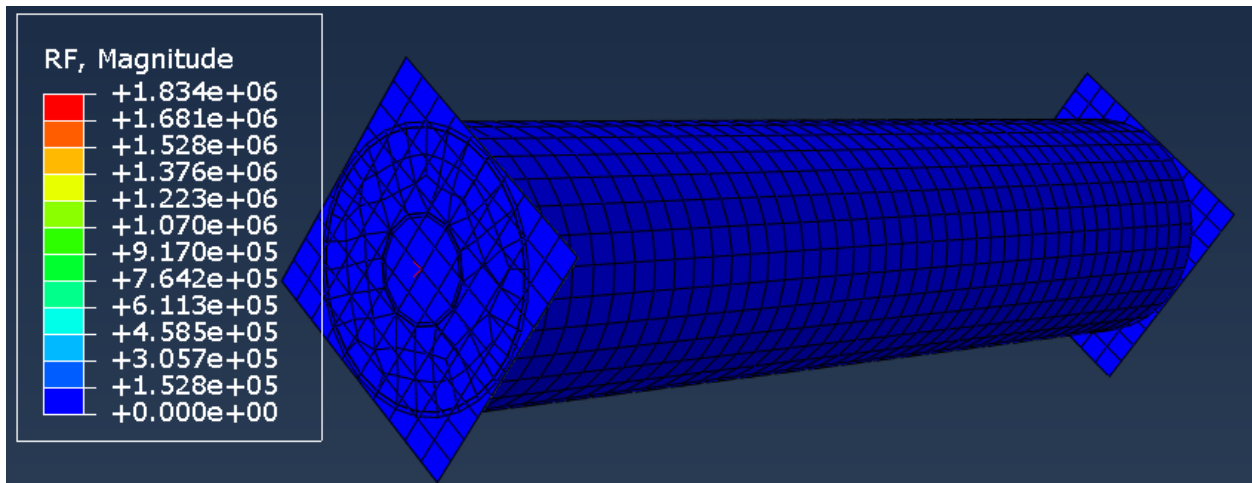


Figure B.8: Axial loads for IST=3mm CFDSSTC column.

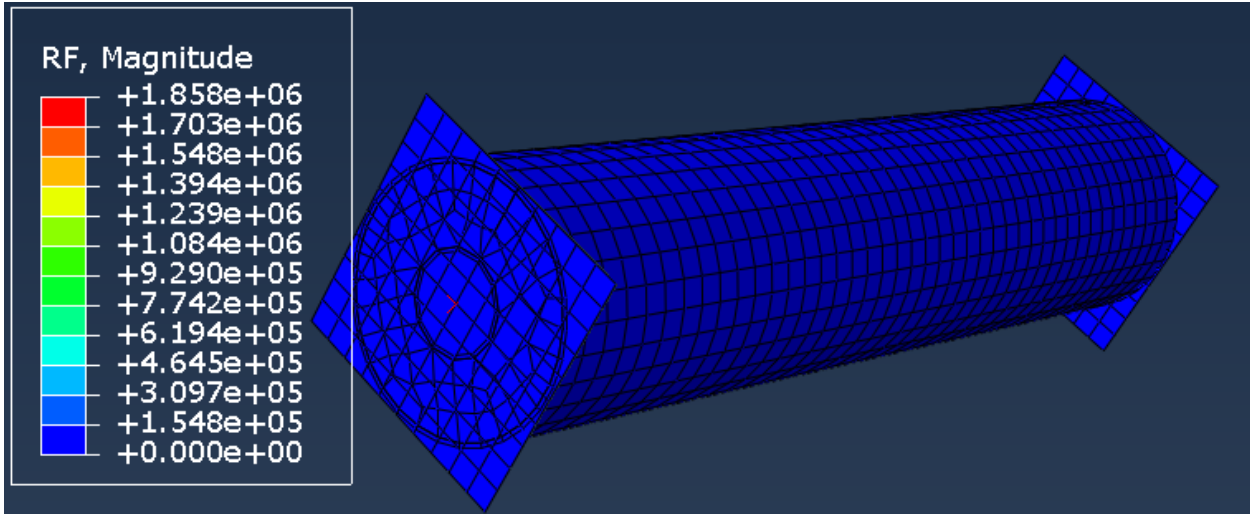


Figure B.9: Axial loads for IST=3.5mm CFDSSTC column.

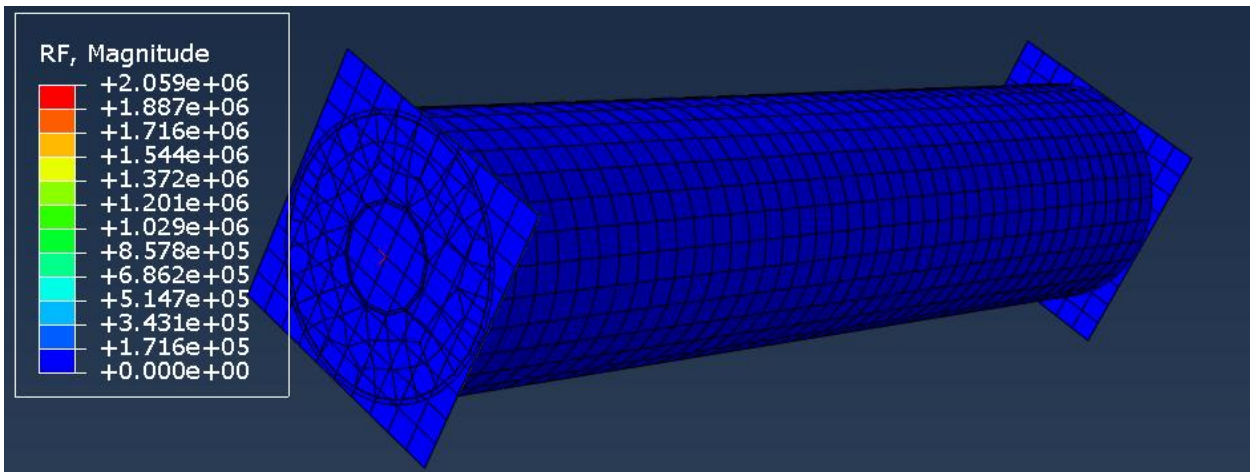


Figure B.10: Axial loads for IST=4mm CFDSSTC column.

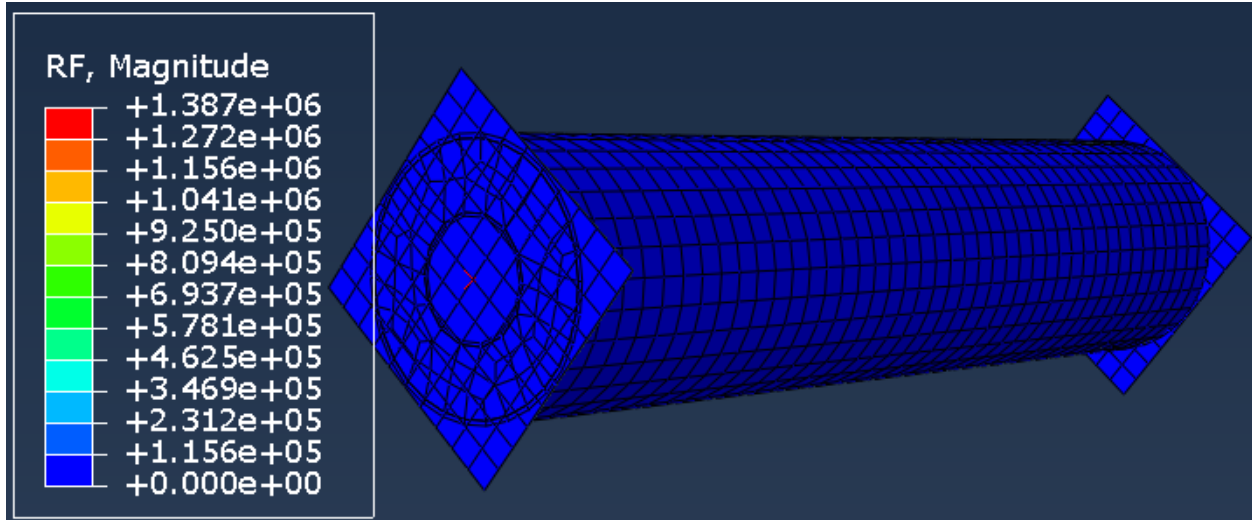


Figure B.11: Axial loads for OST=2mm CFDSSTC column.

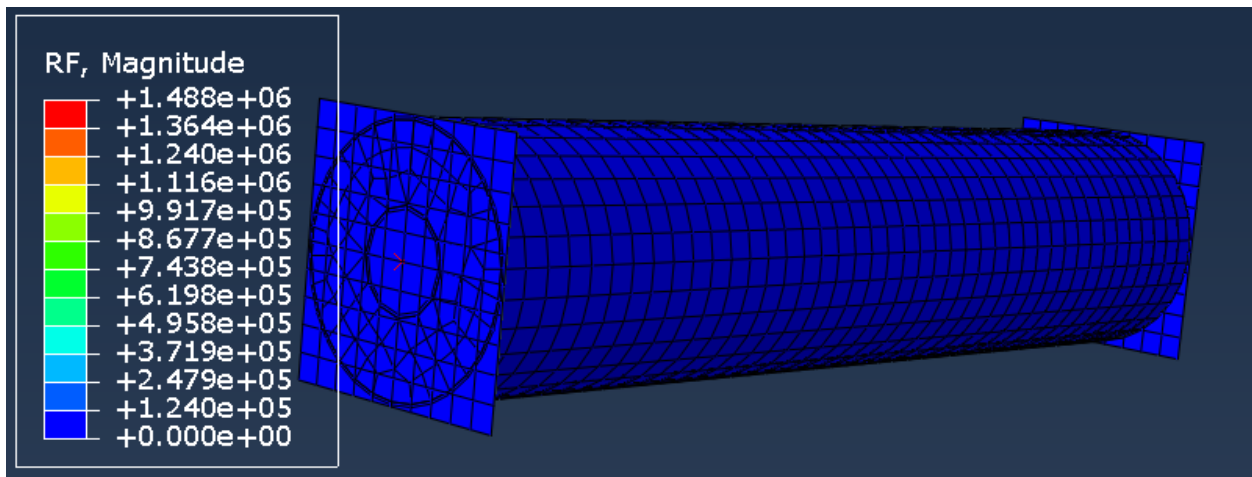


Figure B.12: Axial loads for OST=2.5mm CFDSSTC column.

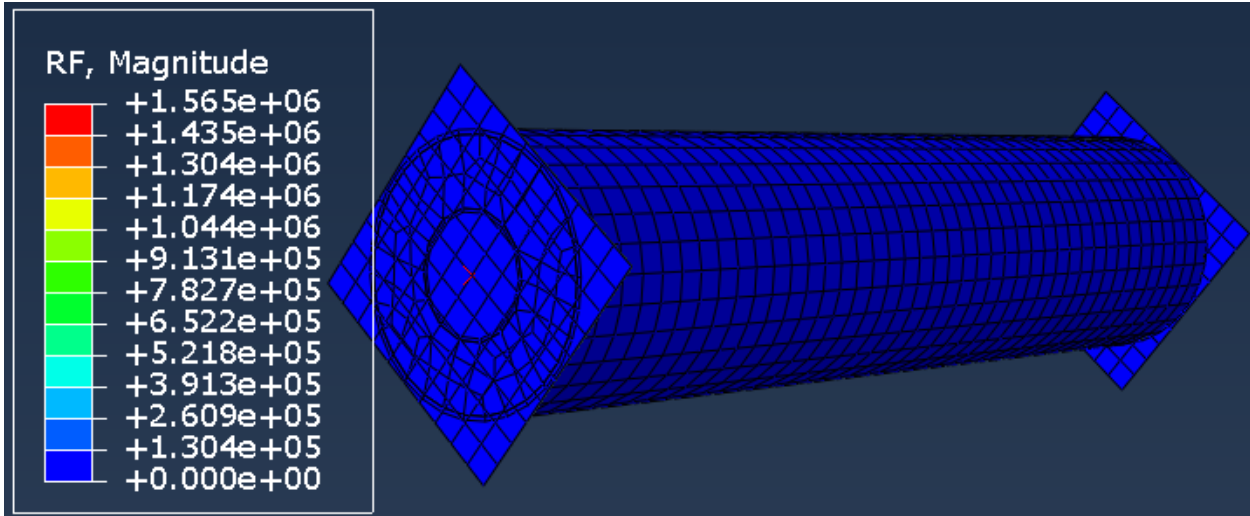


Figure B.13: Axial loads for OST=3mm CFDSSTC column.

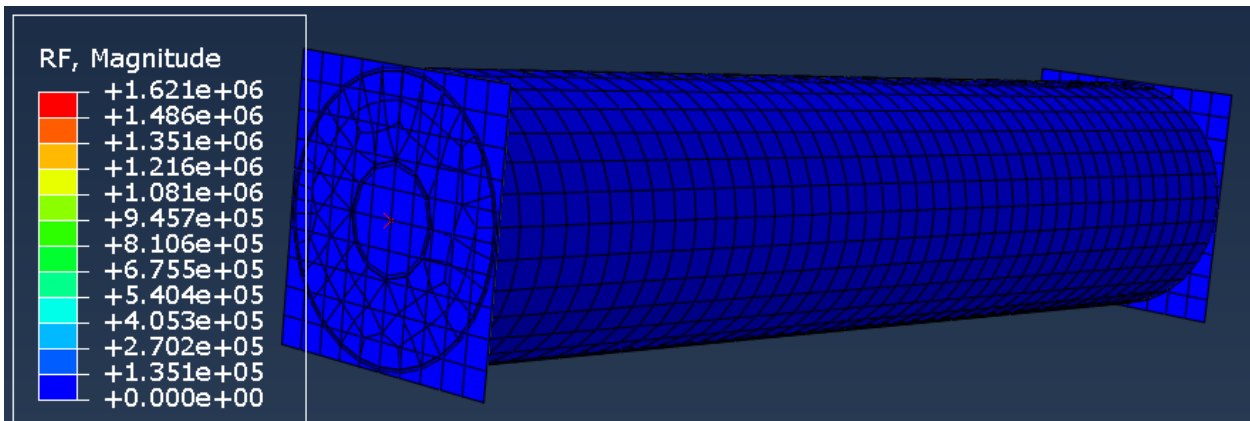


Figure B.14: Axial loads for OST=3.5mm CFDSSTC column.



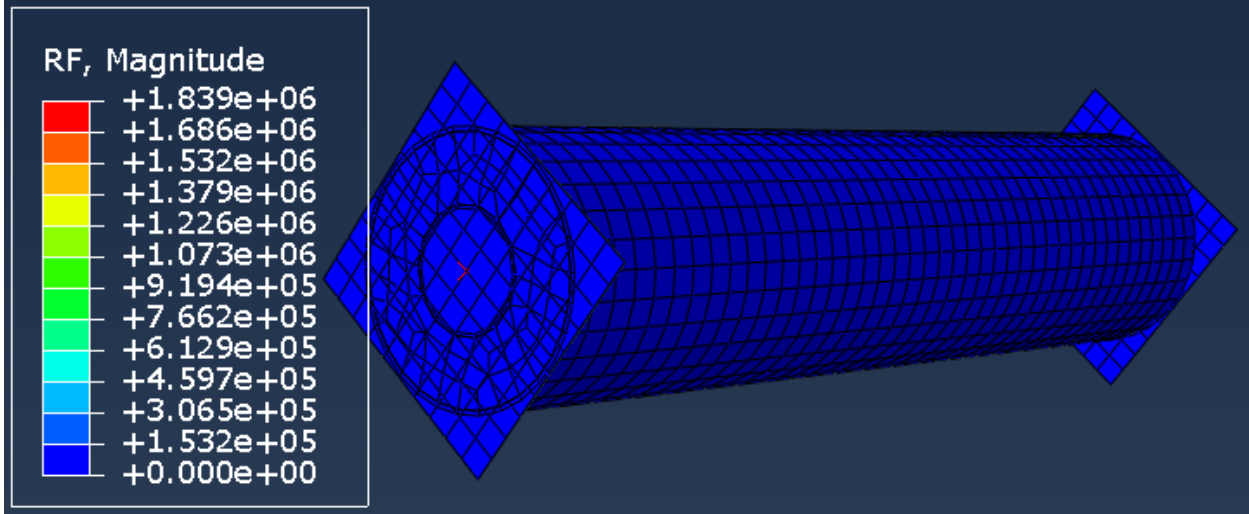


Figure B.15: Axial loads for OST=4mm CFDSSTC column.

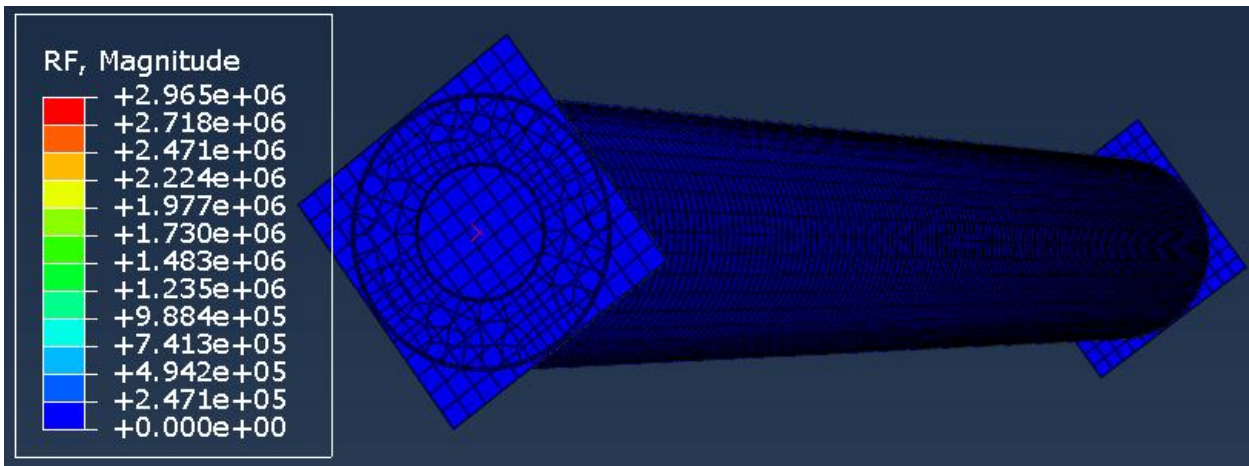


Figure B.16: Axial loads for L=1m CFDSSTC column.

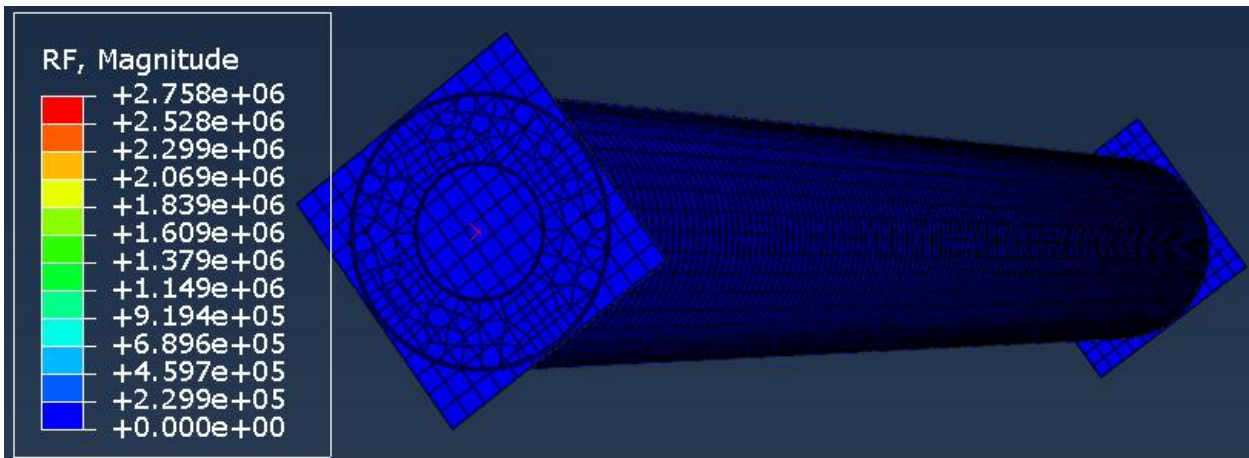


Figure B.17: Axial loads for L=1.5m CFDSSTC column.

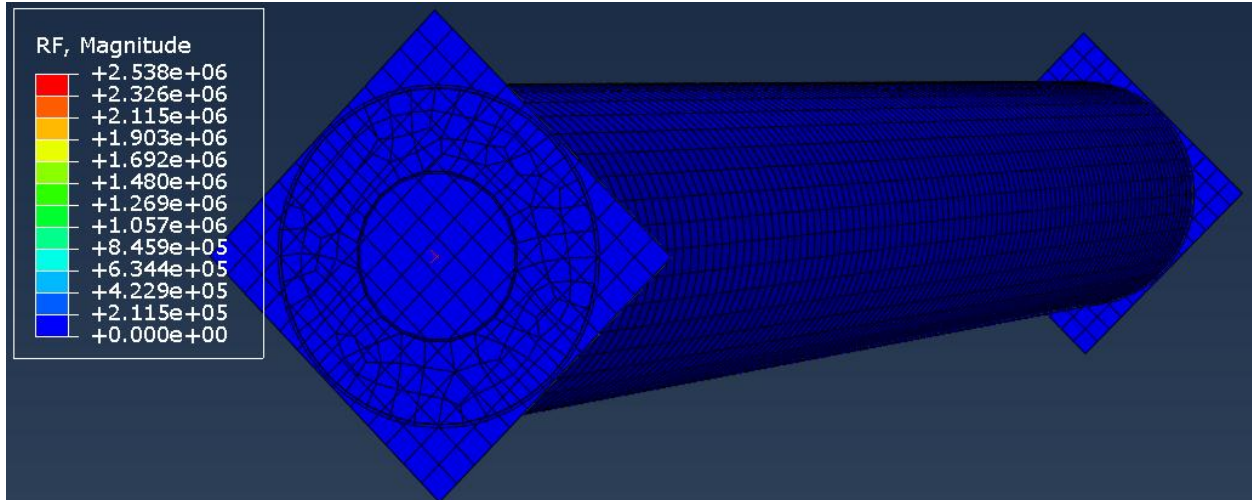


Figure B.18: Axial loads for L=2m CFDSSTC column.

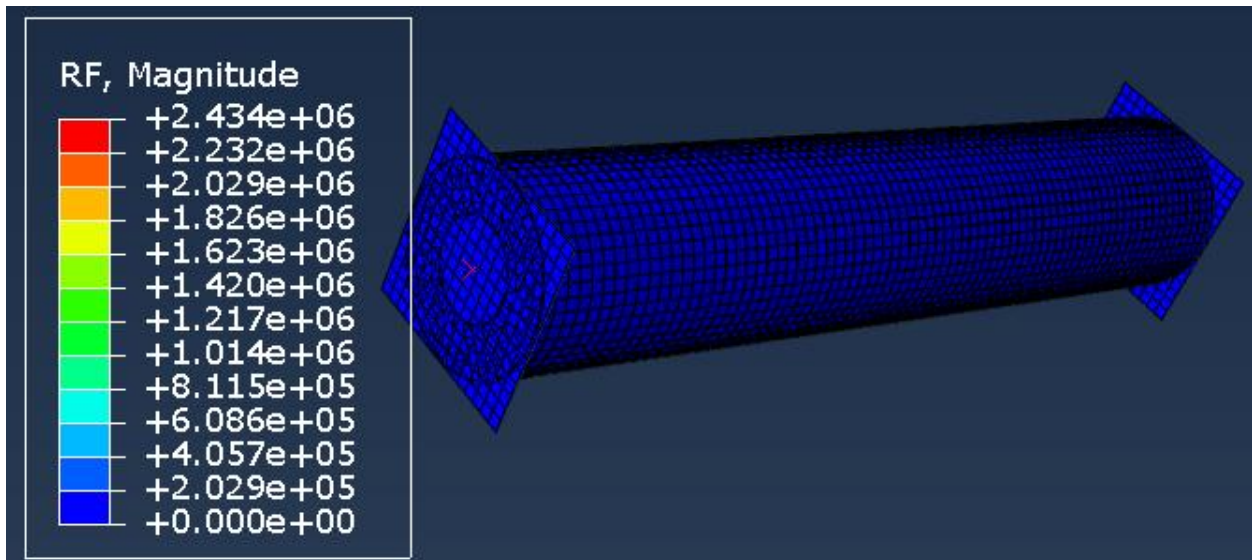


Figure B.19: Axial loads for L= 2.5m CFDSSTC column.

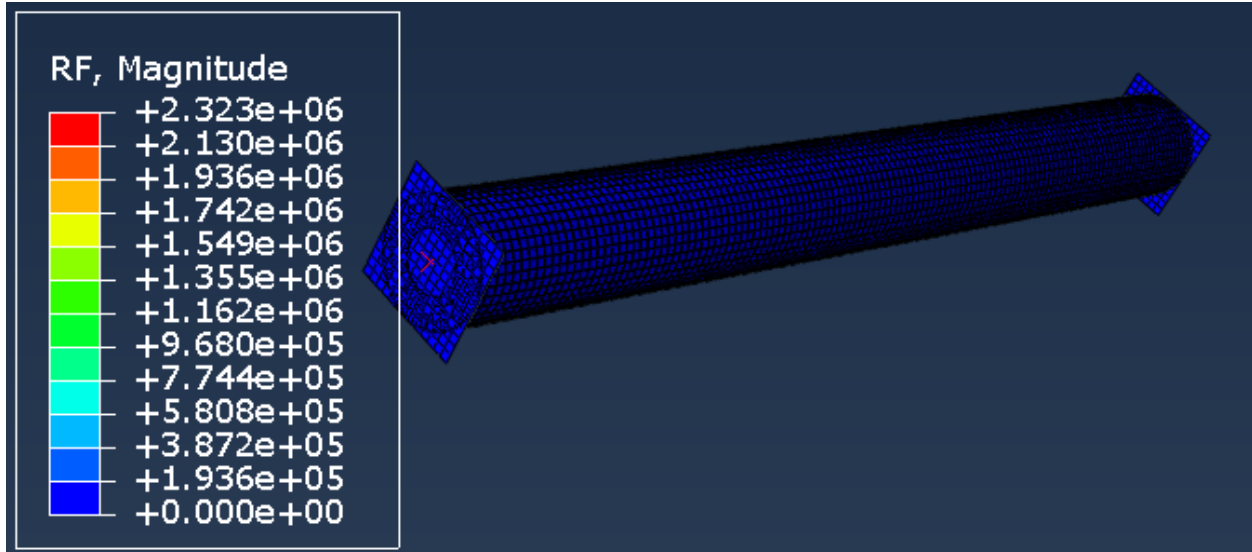


Figure B.20: Axial loads for L= 3m CFDSSTC column.

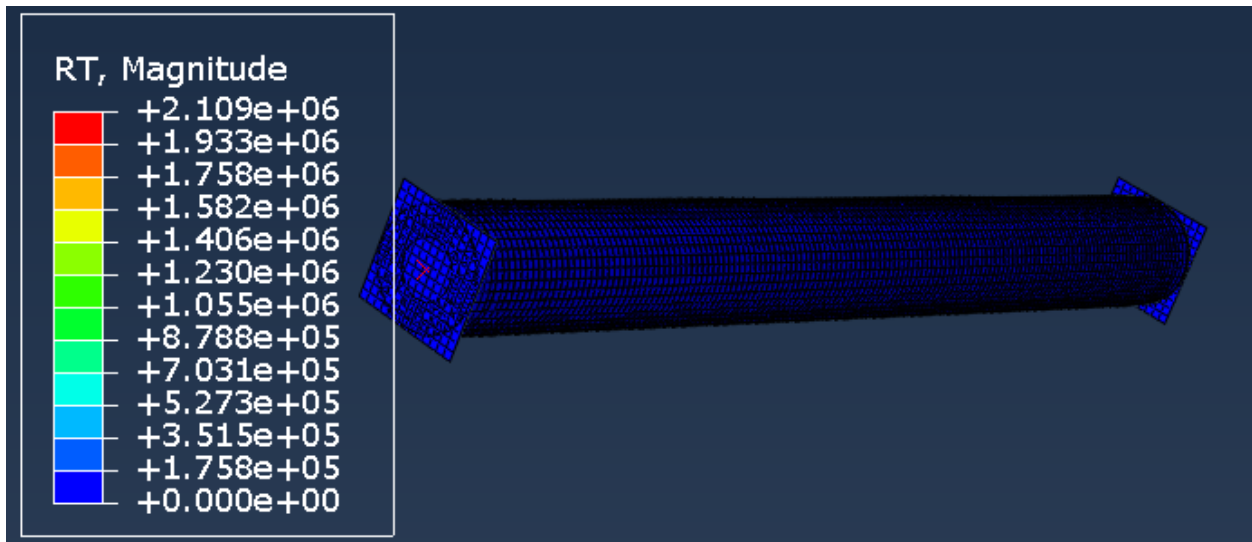


Figure B.21: Axial loads for L=3.5m CFDSSTC column.

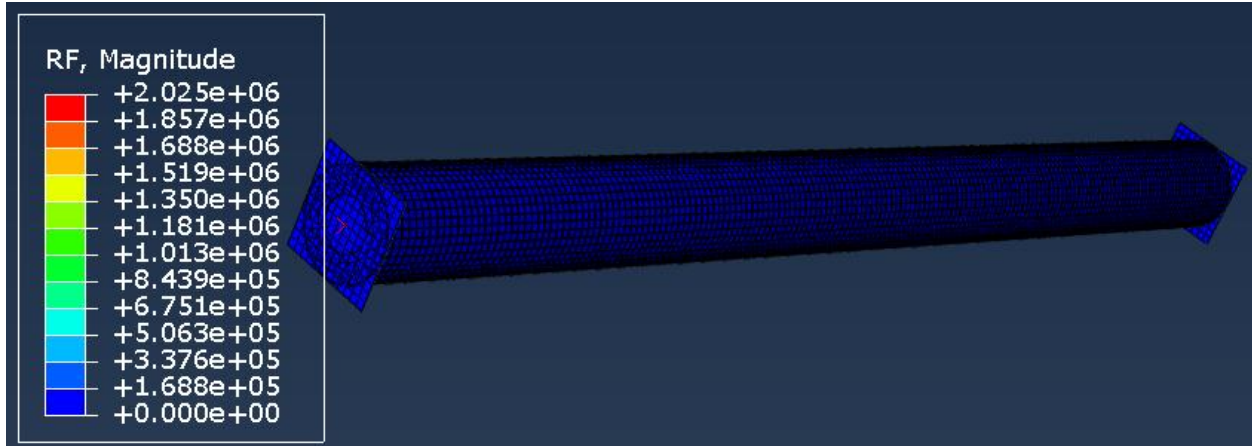


Figure B.22: Axial loads for L=4m CFDSSTC column.

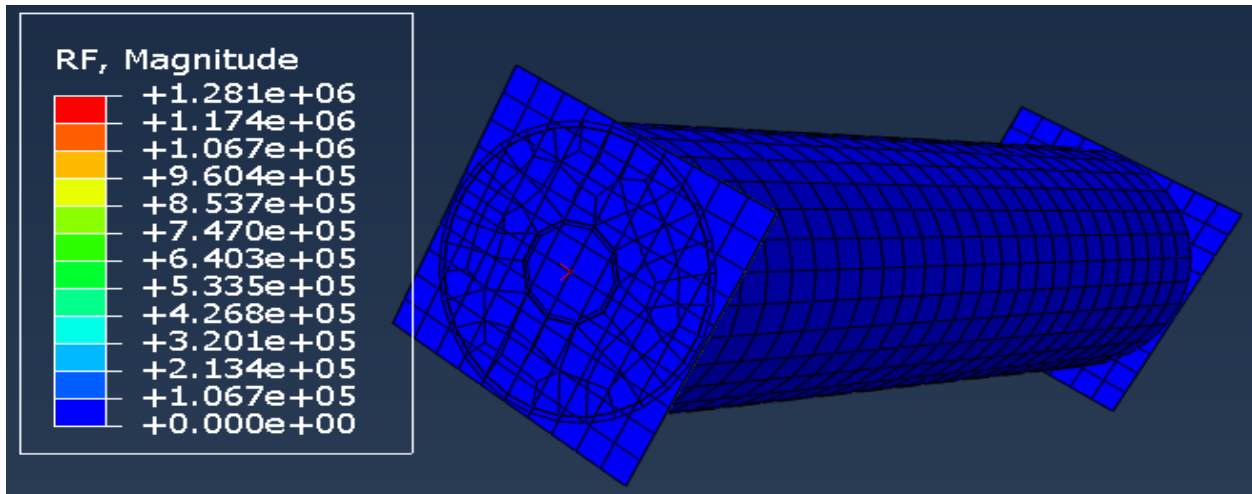


Figure B.23: Axial loads for 0.6m CFDSSTC column.